# Effect of different mutations in the *ATM* gene on the cellular response to ionizing radiation

DISSERTATION ZUR ERLANGUNG DES DOKTORGRADES DER NATURWISSENSCHAFTEN (DR. RER. NAT.) DER FAKULTÄT FÜR BIOLOGIE UND VORKLINISCHE MEDIZIN DER UNIVERSITÄT REGENSBURG


vorgelegt von

Sophie Hinreiner

aus Pößneck


im Jahr 2018

Das Promotionsgesuch wurde eingereicht am: 06.07.2018

Die Arbeit wurde angeleitet von: Prof. Dr. Wolfram Gronwald

Unterschrift:

# Widmung

## Für meine Eltern.

Einmal kommt der Moment, wenn du sagst:

"Nun lass mich schon los. Ich kann selbst fliegen!"

Oh, dann drück ich dich noch einmal geschwind.

Hol tief Luft und geb dir ganz viel Rückenwind.

Leise werde ich beten: "Gott behüt mein Kind!"

Und dann öffne ich meine Arme. Und dann öffne ich meine Arme für dich!

Gerhard Schöne

## In Erinnerung an Conny!

Irgendwann heißt, es kann morgen geschehn
und dass wir uns heut' das letzte Mal sehn.
Drum, was du erlebst, erleb' es total,
denn alles, alles gibt's ein letztes Mal.
Alles, alles gibt's ein letztes Mal.

Gerhard Schöne

# Danksagung

An dieser Stelle möchte ich mich bei allen bedanken, die mich während der Entstehung dieser Arbeit begleitet und unterstützt haben.

Mein besonderer Dank gilt **Prof. Dr. Peter Oefner.** Danke, dass Sie mir die Möglichkeit gegeben haben am Institut für Funktionelle Genomik zu promovieren, Ihre Unterstützung während der gesamten Zeit, die Übernahme des Zweitgutachtens und die Möglichkeit mich durch die Teilnahme an verschiedensten Kursen und Kongressen weiterzubilden.

Ein großer Dank geht an **Prof. Dr. Wolfram Gronwald**. Danke, für die Erstbetreuung meiner Dissertation, deine Geduld und dass du immer ein offenes Ohr für mich hattest.

Einige Betreuer haben diese Arbeit begleitet, u.a. **Dr. Anne Hartmann** und **Dr. Christoph Möhle**. Auch Euch ein großes Dankeschön. Hier gebührt jedoch der größte Dank **Dr. Yvonne Reinders und Dr. Jörg Reinders**. Danke, für eure warmherzige und intensive Betreuung, für die Hilfe bei gefühlt hunderten Western Blots, dem Analysieren riesiger Datensätze und eure Unterstützung, sei es im Labor oder auch privat! Meinen lieben Kolleginnen aus der Proteomics-Gruppe – **Anja Thomas, Corinna Feuchtinger und Dr. Nadine Aßmann** – ebenfalls ein großes Danke! Danke, für unzählige lustige Stunden im Labor, schöne Gespräche und die tolle Zusammenarbeit. Und ganz besonders dir – liebe Nadine – ein liebevolles Danke! Danke, für unsere wunderbare Freundschaft, die selbst über 1700 Kilometer besteht!

Desweitern möchte ich mich bei **PD Dr. Katja Dettmer** bedanken. Danke, liebe Katja für die schöne Zeit in unserem gemeinsamen Büro, deine direkte und offene Art und deine Unterstützung! Und auch hier ein großes Danke an die lieben Kollegen aus der Metabolomics-Gruppe – **Dr. Hanne Kaspar, Dr. Martin Almstetter, Nadine Nürnberger, Dr. Magdalena Waldhier, Dr. Christian Wachsmuth und Dr. Axel Stevens.** Danke, für gute Musik, viel Spaß, tolle Gespräche und den ein oder anderen Kaffeerunden-Plausch!

Ein weiteres Dankeschön geht an die Kollegen der NMR-Grupp von **Prof. Dr. Wolfram Gronwald** – **Claudia Samol, Dr. Matthias Klein, Dr. Helena Zacharias und Jochen Hochrein**. Danke, für die tolle Zeit am Institut.

Nicht unerwähnt bleiben dürfen die Mitglieder der Arbeitsgruppe von **Prof. Dr. Rainer Spang**. Hier insbesondere **Dr. Claudio Lottaz, Dr. Katharina Meyer, Dr. Christian Hundsrucker, Dr. Franziska Taruttis** und – ganz besonders – **Christian Kohler**, der mir bei allen Computerproblemen immer hilfreich zur Seite stand.

Ebenfalls ein großes Dankeschön an unsere guten Seelen des Instituts – **Sabine Botzler** und **Eva Engl**. Danke, für eure stetige Hilfe und Unterstützung in allen Lebenslagen!

Bedanken möchte ich mich auch bei den Kollegen vom Kompetenzzentrum für Fluoreszente Bioanalytik – **Dr. Thomas Stempfel, Dr. Christoph Möhle, Jutta Schipka** und **Susanne Schwab**. Danke, für das Annehmen vieler, vieler Pakte und die netten Gespräche!

Diese Danksagung wäre nicht vollständig ohne ein großes Dankeschön an Sven Schirmer. Auch wenn wir jetzt getrennte Wege gehen - Danke, dass du mich ein großes Stück dieses Weges begleitet hast.

Es gibt noch viele Menschen, die diesen Weg begleitet und unterstützt haben, auch ihnen Danke ich aus tiefstem Herzen! Erwähnt seien an dieser Stelle u.a. **Franziska Iwanow, Manuela Brenner, Laura Ciuca, Martina Frey, Prof. Dr. Ute Hehr, Julia Pietzner, Dr. Alexander Riechers** und viele, viele mehr!

Aus tiefstem Herzen Danke ich **Daniel Wytrykus**. Danke, dass du an meiner Seite bist, mich begleitest, mit mir lachst und weinst und immer an mich glaubst!

Gewidmet ist diese Arbeit meinen Eltern **Petra und Peter Hinreiner**, sowie meiner Schwester **Res Hinreiner** und meiner Oma **Brigitte Krökel**! Danke, dass ihr immer für mich da seid, für eure Liebe und Unterstützung, euren Glauben an mich und für die „Flügel“ die es mir ermöglichen so weit zu fliegen und für eure „Arme“ die immer für mich offen sind. Aus tiefstem Herzen: Danke!

# 1. Summary

Ataxia Telangiectasia - an autosomal recessive, multisystem disorder - is characterized by progressive cerebellar ataxia, telangiectasia, immune defects and a predisposition to malignancy and was first described in 1926 by Syllaba and Henner (Syllaba, L., Henner, K. 1926). The gene – Ataxia Telangiectasia Mutated (ATM) - was identified on chromosome 11q22-23 and up to now more than 350 different mutations have been described. The ATM protein is a 350 kDa serine-threonine protein kinase that localizes mainly to the nucleus and plays a key role in the repair of DNA double strand breaks that are typically induced by ionizing radiation (IR). ATM is activated after IR-induced double strand breaks occur and subsequently phosphorylates many downstream targets that are involved in DNA damage repair mechanisms and cell cycle control. This activation cascade leads either to cell cycle arrest, repair of the DNA damage or induction of apoptosis. Disturbances in these mechanisms can result in an accumulation of DNA alterations that predispose the damaged cells to malignant transformation.

Since 1991, ATM has been discussed as a susceptibility gene for breast cancer (Swift et al. 1991), in particular the missense mutation c.7271T>G, p.Val2424Gly. For this missense variation a dominant-negative mechanism is described in the literature and in 2006 Waddell used expression profiles to discriminate c.7271T>G carriers from healthy controls (Chenevix-Trench et al. 2002; Waddell et al. 2006).

In the present study proteomics-based approaches in addition to different cell biological and biochemical investigations were used to elucidate the cellular reactions upon ionizing radiation of lymphoblastoid cell lines from A-T patients carrying different ATM-mutations with one AT patient homozygous for c.7271T>G, breast cancer patients heterozygous for c.7271T>G, and healthy controls.

FACS analysis could confirm already published data for a higher susceptibility to cell death and G1 arrest (f.e. (Bakkenist und Kastan 2003) for the cell lines derived from breast cancer patients harboring the heterozygous c.7271T>G variant upon IR. In contrast the Western Blot analysis could not confirm the dominant negative effect that was postulated by Chenevix-Trench and Waddell for the cell lines harbouring the heterozygous c.7271T>G substitution. In contrast to the published data the present study could show that downstream targets of ATM are still phosphorylated upon IR. The pedigree of the family A published 2002 by Chenevix-Trench shows that the breast cancer is inherited within the same haplotype, so there could be other factors accounting for this phenotype.

Two proteomics-based approaches, DIGE analysis and SWATH acquisition, were used to investigate the cellular response upon ionizing radiation for all cell lines. Two members of the ATM pathway –SMC1A and MRE11 – were significantly downregulation in the healthy control cell lines, with MRE11 also downregulated in the AT cell lines. A shift in the 2D gel of the

phosphorylated proteins SMC1A and MRE11 would explain that downregulation upon irradiation. Additionally, the AT patients and control cell lines showed an upregulation of RAD23B – a protein involved in Nucleotide Excision Repair (NER) – upon IR in the SWATH approach, which was not present in the cell lines derived from breast cancer patients. The upregulation of RAD23B was also found in the AT patient cell line in the DIGE analysis. This regulation of RAD23B gives a first hint to a restricted function of NER and maybe DNA mismatch repair (MMR) in the cell lines derived from the breast cancer patients harbouring the c.7271T>G substitution. Additionally, the SWATH-MS approach showed a reduced regulation of proteins involved in NER and MMR in the c.7271T>G heterozygous cell lines compared to the controls. Therefore, these proteomics data show for the first time the postulated link between ATM and the MMR pathway ( (Romeo et al. 2011), which needs further investigation.

# 2. Zusammenfassung

Ataxia telangiectasia ist eine autosomal-rezessive vererbte Multisystemerkrankung, welche durch eine fortschreitende zerebelläre Ataxie, Teleangiektasien, Immundefekte und eine Prädisposition für Tumore gekennzeichnet ist. Sie wurde erstmals 1926 von Syllaba und Henner (Syllaba, L., Henner, K. 1926) beschrieben. Das Gen - Ataxia Telangiectasia Mutated (ATM) - liegt auf Chromosom 11q22-23 und bisher wurden mehr als 350 verschiedene Mutationen beschrieben. Das ATM-Protein ist eine 350 kDa Serin-Threonin-Proteinkinase, die hauptsächlich im Zellkern lokalisiert ist. ATM spielt eine Schlüsselrolle bei der Reparatur von DNA-Doppelstrangbrüchen, welche vor allem durch ionisierende Strahlung (IR) induziert werden. IR induzierte Doppelstrangbrüche führen zu einer Aktivierung von ATM, welches dann weitere Proteine - die an DNA-Reparaturmechanismen und Zellzykluskontrolle beteiligt sind – phosphorylieren kann. Diese Aktivierungskaskade führt entweder zum Zellzyklusarrest, zur Reparatur der DNA-Schäden oder zur Apoptose. Defekte in diesen Mechanismen können zu einer Anhäufung von Mutationen führen und somit zu einer möglichen Tumorentstehung beitragen.

Seit 1991 wird ATM als möglicher Risikofaktor für Brustkrebs diskutiert (Swift et al. 1991), insbesondere die Missense-Mutation c.7271T> G, p.Val2424Gly. Für diese Missense-Variante wird in der Literatur ein dominant-negativer Effekt beschrieben, und Waddell verwendete 2006 Expressionsprofile, um Mutationsträger der c.7271T>G-Variante von gesunden Kontrollen zu unterscheiden (Chenevix-Trench et al. 2002; Waddell et al. 2006).

In der vorliegenden Arbeit wurden neben verschiedenen zellbiologischen und biochemischen Untersuchungen auch Proteomik-basierte Ansätze verwendet, um die zelluläre Reaktion verschiedener lymphoblastoider Zelllinien (AT-Patienten mit verschiedenen ATM-Mutationen, eine AT-Patient homozygoten für c.7271T>G, Brustkrebspatienten heterozygot für c.7271T> G und gesunde Kontrollen) auf ionisierende Bestrahlung zu untersuchen.

Mittels FACS - Analysen konnte für die Zelllinien der Brustkrebspatienten nach Bestrahlung eine höhere Sterberate der Zellen sowie ein Arrest in der G1-Phase des Zellzyklus nachgewiesen – und somit bereits publizierte Daten (u.a. Bakkenist und Kastan 2003) bestätigt – werden. Die ebenfalls durchgeführten Western Blots konnten den dominanten negativen Effekt, den Chenevix-Trench und Waddell für die heterozygote c.7271T> G Substitution postulierten, nicht bestätigen: Im Gegensatz zu den publizierten Daten konnte die vorliegende Arbeit zeigen, dass Downstream-Targets von ATM nach Bestrahlung weiterhin phosphoryliert werden. Der Stammbaum der Familie A, der 2002 von Chenevix-Trench veröffentlicht wurde, zeigt, dass der Brustkrebs innerhalb des gleichen Haplotyps vererbt wird, so dass auch andere Faktoren für diesen Phänotyp verantwortlich sein können.

Um die zelluläre Reaktion auf ionisierende Bestrahlung bei allen Zelllinien zu untersuchen wurden zwei Proteomik-basierte Ansätze, DIGE und SWATH, verwendet. Zwei Downstream-

Targets von ATM -SMC1A und MRE11- waren in den gesunden Kontrollzelllinien signifikant herunterreguliert, wobei MRE11 ebenfalls in den AT-Zelllinien herunterreguliert war. Eine möglicher Erklärung hierfür ist eine Phosphorylierung von MRE11 und SMC1A und demzufolge eine Verschiebung der Proteinspots auf dem 2D-Gel. Zusätzlich zeigten die Zelllinien der AT-Patienten und Kontrollen eine Hochregulation von RAD23B - einem Protein, das am Nucleotide Excision Repair (NER) Signalweg beteiligt ist. Diese Regulation konnte jedoch bei den Zelllinien der Brustkrebspatienten nicht nachgewiesen werden. Zusätzlich konnte eine Hochregulation von RAD23B auch in den Zelllinien der AT-Patienten mittels DIGE beobachtet werden. Dies ist ein erster Hinweis auf eine eingeschränkte Funktion des NER-Signalwegs und möglicherweise auch des MMR-Signalwegs in den Zelllinien der Brustkrebspatienten. Zusätzlich zeigten die SWATH-MS-Daten für die Zelllinien der Brustkrebspatienten eine reduzierte Regulation von Proteinen, die am NER- und MMR-Signalweg beteiligt sind. Mittels dieser Proteomdaten konnte erstmals die bereits publizierte Verbindung zwischen ATM und dem MMR-Signalweg ((Romeo et al. 2011)) auf zellulärer Ebene nachgewiesen werden, was durch weitere Experimente näher untersucht werden sollte.

# 3. Introduction

## 3.1. Ataxia Telangiectasia

The central theme of my thesis concerns Ataxia Telangiectasia (A-T), a rare autosomal recessive disorder, the symptoms of which were first described in 1926 by Syllaba and Henner (Syllaba, L., Henner, K. 1926). Fifteen years later, Louis-Bar reported a family with related symptoms, before Boder and Sedgwick recognized A-T as a distinct clinical entity in 1957 (BODER und SEDGWICK 1958; Louis-Bar 1941).

A-T is characterised by a complex phenotype involving the nervous, immune and reproductive systems. A-T patients show progressive cerebellar ataxia, oculocutaneous telangiectasia, radiosensitivity and a predisposition to lymphoid malignancies and immunodeficiency. In Germany, there are approximately 200 reported cases, which corresponds to an estimated prevalence of 1:400,000.

Classical A-T is diagnosed in children between ages one and four years who show progressive cerebellar dysfunction, that can be present as gait and truncal ataxia, head tilting, slurred speech and oculomotor apraxia. The diagnosis is confirmed by measuring the serum-alpha-fetoprotein (AFP) level, which is elevated > 10 ng/mL. Also commonly used is the colony survival assay – a radiosensitivity assay that determines the survival rate of cultured lymphoblastoid cells from A-T patients after irradiation with 1 Gy (Sun et al. 2002) – or karyotyping to determine chromosomal breaks or translocations, like the common 7;14 translocation. The most sensitive and specific test for establishing a diagnosis of A-T is immunoblotting of the ATM protein (Chun et al. 2003). About 90% of the patients do not show detectable ATM protein in this test, around 10% have trace amounts of protein and ~1% show normal ATM protein levels but no kinase activity (so called “kinase-dead”). To measure the activity of the ATM protein usually immunoblotting for ATM-dependent phosphorylation target proteins such as p53 (Ser15), SMC1 (Ser966) or ATM itself (Ser1981) is employed. Therefore, lymphoblastoid cells isolated from A-T patients are irradiated to generate DNA double-strand breaks and, consequently, to activate ATM. After an incubation period of 30 – 60 min, the cells are harvested and the phosphorylation status of the downstream substrate is determined. In 2008 and 2009, two groups described a new method to measure the phosphorylation of H2AX or SMC1 by flow cytometry (Nahas et al. 2009; Porcedda et al. 2008). Another way to validate the A-T diagnosis is sequence analysis to find the underlying mutation in the *ATM* gene.

Classical A-T symptoms vary slightly in the late stages of the disease. However, the time of onset and rate of progression of symptoms can vary considerably. The presenting symptom in classical A-T patients is progressive ataxia, which manifests itself when the child begins to walk. Patients show an ataxic gait and truncal movements and become confined to a wheelchair by the end of the first decade of their life. The speech becomes slurred and they are not able to follow an object across visual fields (oculomotor apraxia). These neurological

symptoms are due to the progressive cortical cerebellar degeneration that involves mainly the Purkinje and granular cells. The second presenting symptom is telangiectasia, which has a later onset and is usually observed between two and eight years of age. The dilation of small blood vessels occurs commonly in the eyes and also in the skin – mainly in the butterfly area of the face - and in the ears (BODER 1985). Compared to the neurological features, the immunodeficiencies vary much more and are present in 60% - 80% of cases. Affected patients suffer an excess of bacterial sinopulmonary infections like sinusitis, bronchitis, pneumonia and later on pulmonary fibrosis. The serum concentrations of IgA, IgE and IgG2 are reduced and the patients show peripheral lymphopenia and a small embryonic-like thymus (McFarlin et al. 1971; McFarlin et al. 1972). Gamma/delta T-cell levels are usually elevated which is typical for an incomplete T-cell development. Peterson and Funkhouse proposed that these can be explained by a defect in genetic recombination thus preventing the switch from immature T-cells with gamma/delta chains to mature T-cells with alpha/beta chains (Peterson und Funkhouser 1990). In addition to immunodeficiency, classical A-T patients show a strong predisposition to malignancy. Younger children tend to have acute lymphoblastic leukemia (ALL) of T-cell origin, older children more aggressive T-cell leukemia and older A-T patients show especially ovarian cancer, breast cancer, gastric cancer, melanoma and sarcoma. In addition to these lead symptoms, A-T is also characterized by many additional features that are more variable in their appearance but can help to confirm the diagnosis. These include premature aging with strands of gray hair, endocrine abnormalities, like unusual types of diabetes mellitus (hyperinsulinism, hyperglycemia and no glycosuria or ketosis and peripheral insulin-resistance), growth retardation and hypogonadism. Nevertheless A-T patients show typically a normal intelligence with some learning difficulties due to their slow motor and verbal responses.

Since the 1980$^{th}$ several reports about A-T variants have been published. Patients, for example, show milder clinical symptoms with a later onset (McConville et al. 1996; Stankovic et al. 1998; Saviozzi et al. 2002), a combination of A-T and Nijmegen breakage syndrome symptoms (Curry et al. 1989; Gilad et al. 1998) or atypical symptoms (progressive ataxia but no telangiectasia, normal AFP and immune function) with mutations in the *ATM* gene and changes in ATM kinase activity (Saunders-Pullman and Gatti 2009; Alterman et al. 2007).

## 3.2. *ATM* Gene

The *ATM*-gene consists of 160 kb genomic DNA, which is transcribed in a mRNA with 66 exons and encodes a 350 kDa protein kinase that is mainly located in the nucleus (Uziel et al. 1996).

In 1988, Gatti and colleagues used genetic linkage analysis to localize the Ataxia-Telangiectasia gene on the long arm of chromosome 11 (11q22-23) (Gatti et al. 1988). In 1995, Savitsky et al. identified one gene in this region, which was mutated in all patients with Ataxia-Telangiectasia symptoms – the *ATM*-gene (Ataxia Telangiectasia Mutated) (Savitsky et al. 1995) and about

90% of the ATM sequence variants are detected in the coding region of the gene. Classical A-T phenotypes are associated with homozygosity or compound heterozygosity for two deleterious *ATM* mutations (Gatti et al. 1999).

To date there are 706 different mutations known (The Human Mutation Database; 03.2013) and 32% of them are nonsense or missense mutations that can lead to a premature degradation or destabilisation of the resulting protein. 27% of the mutations are small deletions, insertions or indels. There are 95 different mutations known to affect splice or regulatory sites of the *ATM* gene, which may give rise to "leaky splicing" whereby a small amount of intact ATM protein is expressed. The remaining 27% are gross deletions, insertions, duplications or complex rearrangements.

## 3.3. ATM protein

The ATM protein is a serine/threonine protein kinase that is evolutionarily conserved and related to the PI3K-like protein kinase family (Phosphatidylinositide-3-kinase; PIKKs). All these proteins are grouped together based on similarities of a conserved domain in their C-terminus. In addition to ATM, two other PIKK family members show substantial sequence similarity and related functions – ATR (Ataxia Telangiectasia and Rad3 related) and DNA-$PK_{CS}$ (DNA-Phosphatidylinositide kinase) (Durocher und Jackson 2001). Low resolution cryoelectron microscopy data of DNA-$PK_{cs}$ showed tandem HEAT repeats in the N-terminus that form a ring-like structure with a "head or crown-like" structure on top of it. This "crown" contains the FAT, PI3-kinase and FATC domain and the ring-like structure has a cavity that can accommodate the ends of a DNA molecule. The N-terminus is an important interaction surface of ATM, for example for NBS1 or chromatin. FAT and FATC domain - that are located in the C-terminus – are involved in the regulation of the kinase activity of PIKKs. The FAT domain can interact with the PI3 kinase domain to stabilize the C-terminal region of ATM itself and is also a hot spot for posttranslational modifications like acetylation, phosphorylation or sumolyation. The PI3 kinase domain is located close to the C-terminus between the FAT and FATC domain. This region has a protein kinase activity and phosphorylates a large subset of proteins especially on ST/Q motifs (Llorca et al. 2003; Rivera-Calzada et al. 2005). One of the first substrates of ATM to be identified *in vitro* and *in vivo* was p53. The stabilization and activation of p53 is defective in A-T patients, which leads to a defective $G_1$-S-checkpoint (Kastan et al. 1992).

More recently, it has been proposed that ATM functions as a redox sensor and may regulate global cellular responses to oxidative stress or a non-nuclear function as a member of the $NF_{\kappa}B$-pathway and an association with peroxisomes and endosomes (Wu et al. 2006; Lim et al. 1998; Watters et al. 1999; Guo et al. 2010). But the most common and best investigated function of the ATM protein is its role in the DNA damage machinery, the control of the cell cycle and the involvement in apoptosis.

The activation of ATM occurs after DNA damage in a MRN (MRE11-RAD50-NBS1)-dependent manner, the ATM dimer is separated in monomers and many posttranslational modifications occur (Bakkenist und Kastan 2003). MRN is a complex of three different proteins, namely MRE11, NBS1 and RAD50; it is required for optimal induction of ATM kinase activity. NBS1 binds with the forkhead-associated (FHA) and the BRCA1 C-terminus (BRCT) domain directly on the active histone H2AX (γ-H2AX) to recruit the MRN complex via binding of MRE11 to the site of the DNA damage (Jager et al. 2001; Paull und Lee 2005). Also ATM is arriving at the DNA damage site through the interaction with MDC1, which forms an interaction platform by binding γ-H2AX via its BRCT domain, ATM via its FHA domain, NBS1 and other downstream targets (Lou et al. 2006). It is likely that ATM is activated at least partially through the initial relaxation of the chromatin structure by the break. But for complete activation ATM has to be localized to the DNA double strand break and it undergoes several posttranslational modifications (Berkovich et al. 2007). In 2003, Bakkenist and Kastan first showed the autophosphorylation on Ser1981 and monomerization of ATM as an important step in the activation process (Bakkenist und Kastan 2003). Therefore, the detachment of protein phosphatase 2 (PPA2) is needed and the following auto-phosphorylation is responsible for the dissociation of the dimeric inactive ATM to an active monomeric form. In 2006, Kozlov et al. showed the functional significance of two other phosphorylation sites in ATM – Ser367 and Ser1893 (Kozlov et al. 2006). But beside these phosphorylation sites, Sun et al. could demonstrate that ATM also undergoes acetylation by the TIP60 histone acetyltransferase at the Lys3016 residue (Sun et al. 2007; Sun et al. 2005). The fully activated ATM is able to phosphorylate a series of downstream targets that are involved in DNA repair, cell-cycle checkpoint activation and transcription. The first substrate of ATM was published in 1998 by three different groups (Banin et al. 1998; Canman et al. 1998; Khanna et al. 1998). They could show that the activated ATM is able to phosphorylate the tumor suppressor p53 on Ser15 in response to DNA damage. ATM also phosphorylates the p53-asccoiated protein HDM2 (human double minute-2) on Ser403 and mediates the CHK2 (checkpoint kinase 2) phosphorylation of HDM2 on Ser342 and Ser367. The three phosphorylation events and the auto-polyubiquitination of HDM2 lead to the degradation of HDM2 and the subsequent release and stabilization of phosphorylated and active p53. p53 can lead to growth arrest (via p21, GADD45 or 14-3-3δ), DNA repair (via GADD45, XPC or p48) or apoptosis (via Bax, Fas, Puma or Noxa) (Lavin 2008). Another ATM-dependent downstream event is the phosphorylation of histone H2AX on its C-terminal end in the chromatin regions surrounding DNA double strand breaks. γH2AX foci are initially present as small compact structures, close to the DNA damage and quickly spread along the chromatin up to 2 Mb away from the break. They act as an assembly platform to facilitate the accumulation of DNA repair and chromatin remodelling proteins near the damaged site. Ubiquitination by UBC13 – an ubiquitin-conjugating enzyme - mediates the TIP60-dependent acetylation and, therefore, the release of γH2AX from damaged chromatin (Pilch et al. 2003; Ikura et al. 2007). Another substrate of ATM is MDC1, which binds to γH2AX via its BRCT domain and acts as a platform for DNA repair proteins, too. Furthermore, ATM is also required to phosphorylate NBS1 on Ser278 and Ser343

and to mediate the ATM-dependent phosphorylation of SMC1 on Ser957 and Ser966 for activation of the S-Phase checkpoint, cell survival and maintaining the integrity of the genome (Gatei et al. 2000; Kitagawa et al. 2004). Activated ATM and NBS1 are important for the repair process during Homologous Recombination (HR).

## 3.4. Genomic instability

### *3.4.1. DNA damage*

The DNA is a rich source of genetic information in each living cell and its integrity and stability is essential for life. DNA damage is unavoidable and arises by spontaneous alterations of the chemical bonds in the DNA through endogenous cellular processes like copying errors introduced by DNA polymerase, oxidations or hydrolysations (deamination, depurination) from reactive oxygen species or exogenous agents like UV-light, ionizing radiation or chemicals. If DNA sequence changes are not repaired, both proliferating and quiescent cells might accumulate mutations and function no longer properly. Thus, the prevention of DNA damage in all types of cells is important for cell survival and several cellular mechanisms for repairing damaged DNA and correcting sequence errors have evolved. Because DNA plays an active and critical role in cell division, the control of DNA repair is closely tied to the regulation of the cell cycle. During the cell cycle, checkpoint mechanisms ensure that the DNA is intact before permitting replication and cell division to occur. Cells developed a number of processes to detect and repair the various types of alterations in the DNA and many of the proteins involved are highly conserved throughout evolution. Alterations in the DNA can range from single base mutations - that affect only one DNA strand - to breaks across both strands of the DNA – so-called double strand breaks.

### *3.4.2. DNA Repair*

For single base mutations there are two common repair ways known. The first one is called Base Excision Repair (**BER**) and is commonly used to repair spontaneous DNA damage that can be caused by free radicals and other reactive species generated by metabolism, for example a deamination of 5-methyl cytosine to thymidine. DNA glycosylases flip the damaged base out of the helix and hydrolyse the bond that connects it to the sugar-phosphate-DNA backbone. An endonuclease cuts the DNA strand and the result is a single-stranded-gap, which is filled and sealed by a DNA polymerase and ligase. Humans have a large number of specific glycosylases and each of them is specific to certain types of base alterations.

The second mechanism to repair point mutations is called Nucleotide Excision Repair (**NER**). This way to repair DNA damage is mainly used to fix DNA regions that contain chemically modified bases, which influence the normal shape of DNA locally, *e.g.*, thymine-thymine-dimers caused by UV-light. Special repair proteins recognize the DNA lesion and recruit

transcription factors that unwind and stabilize the DNA helix. Endonucleases cut the damaged strand on each side of the lesion and release the DNA fragment with the damaged bases. Afterwards, the gap is filled by a DNA polymerase and sealed by a DNA ligase.

Another form of DNA damage are double strand breaks. They are caused by ionizing radiation (including X-ray and gamma-ray) and/or some anticancer-drugs (like bleomycin). These breaks are highly deleterious and an incorrect rejoining can lead to chromosomal rearrangements and translocations, which can produce a hybrid gene or inappropriate activation of genes. An exception is the immune system. The B and T cells are particularly susceptible to DNA rearrangements of their immunoglobulin or T-cell receptor genes. DNA double strand breaks can be repaired through one of the two following mechanisms – Non-Homologous-End-Joining (NHEJ) or Homologous Recombination.

Non-homologous-end-joining (**NHEJ**) uses the fact that the movement of the DNA molecules in the protein-dense nucleus is fairly minimal and so in general the correct broken DNA ends can be joined together. But the repair process results in the loss of genetic material at the joining end and sometimes in translocations, if broken ends from different chromosomes are joined together. The rejoining of the non-homologous ends of two DNA molecules is processed by a complex of Ku- and DNA-dependent protein kinases, which bind to the DNA double strand break. Nucleases remove a few bases to form blunt DNA strands that are ligated by DNA ligases.

In contrast to the error-prone repair by NHEJ, homologous recombination (**HR**) involves reactions between three DNA molecules – the two broken DNA ends and the intact DNA strand from the sister chromatid. Therefore, HR is normally used during and/or after DNA replication, when the sister chromatid is available for use as a template in the repair process. The initial step in the repair of DNA double strand breaks by Homologous Recombination is the end resection in order to generate 3´overhangs, which is normally done by the MRN complex. The 3´-overhangs are coated by the coiled-coils of RAD50 to protect the DNA ends from further resection and prevent the formation of secondary structures. Afterwards, RAD51 binds to the single-stranded DNA ends and searches for the homologous DNA sequence in the sister chromatid. RAD51 mediates the strand invasion and the 3´-overhang is elongated by DNA polymerase that uses the complementary strand in the undamaged homologous DNA as a template. The so-called Holliday junction is processed and resolved by DNA helicases and nucleases. Because this repair mechanism uses the undamaged homologous DNA strand as a template, HR is an error free way to repair DNA double strand breaks.

### *3.4.3. Cell Cycle, Cell Cycle Arrest and Apoptosis/Necrosis*

The **cell cycle** is an ordered series of events a proliferating eukaryotic cell passes through. Two processes have to occur in the cell for it: the doubling of the genomic DNA, which is done in the S-Phase and the halving of the genome during mitosis (M-Phase). The cell cycle consists of

two different stages: the Interphase – starting with the $G_1$-Phase and going through S-Phase to the $G_2$-State – and the M-Phase. After cell division each daughter cell can enter a new cycle or can leave the cycle and stay in the $G_0$-Phase – a resting stage, which is common for fully differentiated cells (*e.g.*, neurons).

During the $G_1$-Phase the cells synthesize RNAs, proteins and increase in size, before they replicate the DNA in the S-Phase. This is followed by a second G-Phase ($G_2$), in which the cells continue to grow and synthesize additional proteins. In the subsequent M-Phase the eukaryotic cells separate into two similar daughter cells. This phase is sub-divided into four stages – prophase, metaphase, anaphase and telophase - finished by cytokinesis. In eukaryotic cells, special proteins are involved in controlling the cell cycle – cyclin-dependent-kinase-complexes. These complexes are composed of a regulatory cyclin subunit and a catalytic cyclin-dependent-kinase (CDK) subunit.

At the transition between the $G_1$/S-phase and the $G_2$/M-Phase and at the end of the S-Phase, there are checkpoints that monitor the integrity of the specific cell cycle event before progressing into the next phase. UV-light, ionizing radiation, chemicals and other endogenous or exogenous agents can cause DNA damage. Before mitosis, DNA damage has to be repaired to avoid the transfer of damaged DNA to daughter cells. The $G_1$/S-checkpoint prevents the replication of damaged DNA-matrices and the $G_2$/M-checkpoint the segregation of damaged chromosomes. The cell cycle checkpoints function as control points to arrest the cell cycle and to determine whether the damage can be repaired and the cells progress in cell cycle or cannot be repaired and the cells have to undergo apoptosis. To stop the cells at these checkpoints, special proteins – checkpoint kinases - are needed to recognize and repair DNA damage as well as to control the cell cycle arrest and the way to apoptosis.

Apoptosis – also called programmed cell death – is the intracellular death program that exactly balances cell division, to ensure that only non-damaged cells divide. Another form of cell death is called necrosis. During necrosis a cell swells and bursts as a result of acute injury causing a potentially damaging inflammation response. During apoptosis, in contrast, the cell shrinks and condenses, the cytoskeleton collapses, the nuclear envelope disassembles, and the nuclear DNA breaks up into fragments. All cellular compartments are packed into so-called “apoptotic bodies”, which are phagocytosed either by a neighbouring cell or a macrophage. Leakage of cell content does not occur, thus avoiding the damaging consequences of cell necrosis and allowing the recycling of the cellular components by the ingesting cell (Elmore 2007).

## 3.5. ATM and Cancer

A defective DNA damage repair machinery can lead to an accumulation of DNA breaks and/or mutations in the DNA. The cell cycle can be disturbed, which can lead to an uncontrolled cell division and an increased incidence of cancer.

As already described above, A-T patients are at an increased risk of malignancy and are estimated to have a 100-fold increased risk of cancer compared to the general population (Ahmed und Rahman 2006). The combination of increased cellular radio-sensitivity, cell cycle checkpoint defects and chromosomal instability leads to the development of malign tumors in more than 30% of AT patients. Most AT patients are compound heterozygous for truncating mutations or carry one truncating mutation and one missense mutation. Homozygous carriers are uncommon, except in consanguineous families or in the case of specific founder mutations. Before the *ATM* genes was identified, it was already suggested that the blood relatives of A-T patients (obligate or potential heterozygous *ATM* mutation carriers) have an increased risk of cancer, especially breast cancer (Swift et al. 1991). Easton at al. supported this by the meta-analysis of several studies and estimated the relative risk for breast cancer in AT heterozygotes at 3.9-fold (Easton 1994). But there were also reports that could not find any evidence for an increased risk of *ATM* mutations in breast cancer patients (FitzGerald et al. 1997). In 2006, Renwick et al. tried to resolve the confusion regarding the role of *ATM* mutations in breast cancer susceptibility and published the first case-control study in which they compared the frequency of *ATM* mutations in familial breast cancer vs. controls (Renwick et al. 2006). AT heterozygotes showed an estimated relative risk for breast cancer of 2.37. However, all these studies are inconclusive because of the small number of cases and most of them screened only a part of the *ATM* gene for specific mutations. Nevertheless, together the results from Renwick (case-control study) and Thompson (epidemiological study) indicate a 2-fold risk for breast cancer in AT heterozygotes (Thompson et al. 2005). Only 15% of them will develop breast cancer in their life, compared to BRCA1/2, which have a 15-fold risk of breast cancer and 70% of them will develop breast cancer. Thus, it seems likely that *ATM* is associated with a moderate risk of breast cancer, but it is still not clear if *ATM* mutations can act multiplicatively and in consideration of the cellular radiosensitivity the *ATM* mutation status might influence the response to radiotherapy (Angèle und Hall 2000; Gutiérrez-Enríquez et al. 2004; Meyer et al. 2004). Therefore, future research will be crucial to understand the impact of *ATM* mutations on breast cancer, breast cancer therapy and the role of *ATM* in cell cycle control, DNA repair and cellular radiosensitivity.

## 3.6. Breast cancer

Breast cancer is one of the most commonly diagnosed cancers. It is the second leading cause of cancer death in women. Breast cancer is classified into different types based on histology. The ductal carcinoma starts in the lining of the breast milk ducts. The non-invasive or pre-invasive cancer is called carcinoma *in situ* and during this stage the cancer cells have not spread into the surrounding breast tissue yet. If the cancer cells break through the wall of the duct and grows into the fatty tissue of the breast it is called an invasive ductal carcinoma. At this point, the cancer cells are also able to metastasize. Another form is the lobular carcinoma where the cancer cells originate from the lobules – the milk-producing glands. Like a ductal

carcinoma, it is also able to metastasize in the surrounding tissue. Less common types of breast cancer are, for example, the inflammatory breast cancer – where cancer cells block the lymph vessels of the skin – which looks like an inflammation of the breast skin. Like other cancers, breast cancer is staged by the TNM system, which gives codes to describe the severity of the cancer. This system is based on the size/extent of the primary tumor ('T'), the involvement of nearby lymph nodes ('N'), and the distant metastasis ('M').

There are a few known risk factors for breast cancer such as age (due to a reduced capability to repair DNA damage), environmental and lifestyle factors (radiation to the chest, combined hormone replacement therapy, overweight, nulliparity, late first birth, early menarche and late menopause), and genetic factors. A genetic contribution is indicated by the increased incidence of breast cancer in women with a family history. In the latter case, multiple relatives are affected, they can show an early age of diagnosis, the occurrence of bilateral or multiple ipsilateral breast cancer and sometimes affected male relatives. Based on the risk and frequency, there are currently three breast cancer susceptibility genes or loci recognized. They are classified into high risk genes (*BRCA1* and *BRCA2*), intermediate risk genes (*ATM* and *CHEK2*), and modest-risk genes or loci. Mutations in the high risk genes confer a 5-10-fold increased risk for breast cancer, while for intermediate and low risk loci, respectively, a 2-5-fold and a 1.25-fold increased risk has been recognized.

## 3.7. *ATM* Missense Mutation c.7271T>G

In this part, I will give an introduction to the missense mutation c.7271T>G of the *ATM* gene, which has been studied quite extensively. In 1998, Stankovic (Stankovic et al. 1998) reported the spectrum of different *ATM* mutations in the British Isles. They described three affected members of a family (in the publication this family is referred to as family 109), which showed long-standing ataxia. The index patient had severe truncal ataxia, but could still walk with support at the age of 48 years; slightly peripheral ataxia; oculomotor apraxia; reduced muscle tone and reflexes in arms and legs and progressive dysarthria. She showed only minimal telangiectasia – except on the right breast, as a side effect of a postoperative radiotherapy after an invasive ductal carcinoma (at the age of 44 years), which was treated with lumpectomy and conventional radiotherapy. Four years later, she developed an intraductal carcinoma *in situ* in the contralateral breast, which was treated by lumpectomy only. The brother of the index patient showed abnormal head movements since the age of three years and ataxia with 9 years. His neurological course was similar to that of his sisters, but slightly more severe. The sister of the proband also showed a similar neurological course. Quite unusual for A-T patients, she gave birth to a normal son at age 37, with no history of miscarriage or stillbirth. Like her sister, she also developed an invasive ductal carcinoma of the right breast at the age of 50 years. Interestingly, the mother of the sisters also developed breast cancer at the age of 82 years, but that may have been sporadic. Stankovic could detect a missense mutation in the *ATM* gene for this family and a second family (family 46), which

was the only change in the *ATM* gene that was observed in the family 109. Additionally, this missense change segregates with A-T and breast cancer in both families and showed a mild clinical phenotype with lower a reaction to radiation. This missense mutation was present in a homozygous state in all patients of family 109 and together with a second frameshift mutation in all patients in family 46. The c.7271T>G transition leads to a change from a highly conserved valine to a glycine at position 2424 on the protein level, which changes a large hydrophobic amino acid into a small amino acid. Additional analysis showed an increased number of chromosomal breaks after irradiation of whole blood samples with 1 Gy compared to control cells but not as high as in classical A-T patients. Western Blot analysis revealed a full-length ATM protein for the c.7271 homozygous carriers and compared to heterozygous c.7271 carriers and normal individuals the same amount of ATM protein. In contrast, patients who carry the c.7271T>G missense mutation and the frameshift mutation (members of family 46) had a reduced level of ATM protein compared to control cells in western blot analysis. Stankovic postulated that the detected mutant ATM protein showed residual function and, therefore, a 'dose response' effect, in which the degree of mildness depended on the level of mutant but functional ATM protein. Furthermore, the history of both families showed that female heterozygotes were at an increased risk for breast cancer and this observation raised the possibility that the cancer risk might be higher for certain *ATM* mutations. In 1999, Gatti (Bernstein et al. 2003; Gatti et al. 1999) picked up these assumptions and also put forward a model to explain the apparent contradiction between the epidemiological studies and the case-control comparison of *ATM* in breast cancer. He differentiated between *ATM* missense mutations, which lead to the production of an altered ATM protein, and truncating mutations that result in no or less ATM protein. The truncating mutations are less frequent compared to the missense variants, predispose to AT and may have some cancer predisposing effects but they are not major cancer susceptibility alleles in the general population. In contrast, the altered ATM protein resulting from missense mutations can be incorporated into the protein complex and may thus disrupt the function of this complex, which could result in additional phenotypic effects and the absence or substantial reduction of ATM protein concentration. In 2002, Chenevix-Trench (Chenevix-Trench et al. 2002) screened multiple-case breast cancer families, which were negative for mutations in *BRCA1/2*, a large number of unselected breast cancer patients and controls for two *ATM* mutations, that reportedly increased the risk for breast cancer. One of them was the c.7271T>G transition. The other one was a splice mutation that leads to an incorrect splicing of exon 11 and results in an exon skipping and a truncated ATM protein. They could find one family, in which the heterozygous missense mutation c.7271T>G segregated with breast cancer. They established lymphoblastoid cell lines of all mutation carriers for *in vivo* analysis. After irradiation with 6 Gy, Western Blot analysis revealed full length ATM protein for homozygous carriers of c.7271T>G comparable to control cell lines and c.7271T>G heterozygous carriers. However, additional Western Blot analysis for downstream targets of ATM showed a completely abolished p53 phosphorylation in c.7271T>G homozygous carriers. c.7271T>G heterozygous carriers had only 15-25 % of normal kinase activity – measured by p53 and BRCA1 phosphorylation - compared to normal controls.

Based on these results Chenevix-Trench hypothesized that the c.7271T>G mutation acts in a dominant-negative manner and, therefore, the wild-type enzyme is unable to function normally in the presence of the altered protein, due to competition effects for binding partners, substrates and regulators and, therefore, increases the risk for breast cancer in these women. The hypothesis of mutations with a dominant negative effect was first published by Herskowitz in 1987 (Herskowitz 1987). Interestingly, while the c.7271T>G variant segregates with breast cancer in this family, the affected and unaffected mutation carriers showed a reduced kinase activity compared to the control cell lines and heterozygotes were not radiosensitive *in vitro*.

In 2006, Waddell could identify two additional index cases that carried the c.7271T>G variation and tried to characterize this alteration by gene expression profiling (Waddell et al. 2006). Back in 2002 Watts used gene expression profiling to determine AT carriers and could show that mutation carriers show an "expression phenotype" (Watts et al. 2002), which could be a new approach to identify carriers. They used microarray analysis to compare expression profiles of lymphoblastoid cell lines from AT carriers vs. controls with and without irradiation. 71 genes were identified and four genes (*LIM*, *CDKN2D*, *TFRC* and *ARF6*) could be used to discriminate between AT carriers and controls. However, they did not propose that the expression level of these four genes will allow reliable classification due to small sample size. In 2006, Waddell et al. picked up this approach and based on the hypothesis, that the missense mutation c.7271T>G acts in a dominant-negative manner, they assumed that c.7271T>G carriers would display the same expression and IR sensitive phenotype as truncation mutation carriers and, therefore, would confirm the dominant-negative mechanism of the c.7271T>G missense mutation. They could identify 77 genes by microarray that were overexpressed in heterozygotes and homozygotes c.7271T>G compared to wild-type family members and unrelated controls. All these genes are involved in cell growth and cell maintenance, signal transduction and nucleic acid metabolism, but they could not identify any of the genes Watts et al. had found in their expression study in 2002. Western blot analysis for p53 and phosphorylated p53 (Ser15) were carried out to study radiosensitivity. The heterozygous and homozygous c.7271T>G carriers showed a wide range of response and interestingly in the publication from 2006 Waddell could not confirm the results from 2002 for all cell lines. In contrast to the previously reported results, the phosphorylation of p53 at Ser15 was comparable between the wild-type cell lines and c.7271T>G heterozygotes. The authors justified this discrepancy with the assumption that in the previous study they had used freshly established lymphoblastoid cell lines and that the prolonged *in vitro* culture of the cell lines might have compromised the dominant-negative effect. Nevertheless, the heterozygous c.7271T>G carriers showed higher levels of p53 and phosphorylated p53, which is consistent with most of the reported cultured AT cell lines and might be due to the activation of other cellular DNA damage repair pathways after ionizing radiation. The use of other DNA damage pathways is supported by the observation that c.7271T>G homozygotes show the highest incidence of chromosomal aberrations, followed by heterozygous carriers and, thereafter,

wild-type cells. In 2009, Tavtigian *et al.* picked up the theory of the dominant negative mechanism in c.7271T>G carriers. They developed a strategy to estimate the risk attributable to rare missense variants on susceptibility genes for breast cancer to improve the power of case-control mutation screening studies. Therefore, they screened data of seven published ATM case-control studies and could show that rare missense variations – that are in the last third of the ATM protein – confer an increased risk of breast cancer. Additionally a subset of these missense mutations confer a higher risk for breast cancer than classical AT mutations, which resembles the hypothesis of Gatti in 1999 (Bernstein et al. 2003; Gatti et al. 1999). Gatti proposed that these ATM variations are common in the general population, whereas Tavtigian hypothesizes that the high-risk variations in the FAT-, kinase and FATC-domain of the ATM protein are very rare in the population. They also note that relatively common *ATM* missense mutations individually confer a moderately increased risk for breast cancer. Therefore, it is very important to complement these bioinformatics and statistical results with functional assays to reclassify these missense variations as clearly or likely pathogenic in matters of breast cancer susceptibility.

## 3.8. Motivation

Ataxia Telangiectasia is an autosomal recessive, multisystem disorder characterized by progressive cerebellar ataxia, telangiectasia, immune defects and a predisposition to malignancy. It has an estimated prevalence of 1:400,000 and a heterozygous frequency of 1% in the general population. The gene mutated in this disease was identified on chromosome 11q22-23 and named *Ataxia Telangiectasia Mutated* (*ATM*). To date, more than 350 different mutations have been described that are distributed over the entire gene. More than 70% of the mutations are truncating mutations that lead to a destabilization of the resulting protein. The ATM protein is a 350 kDa serine-threonine protein kinase that localizes mainly to the nucleus. It plays a key role in the repair of DNA double strand breaks that are typically induced by ionizing radiation, thereby activating ATM. ATM in turn activates many downstream targets such as DNA damage repair mechanisms by SMC1 or CHK2 and the p53-pathway leading either to cell cycle arrest, the repair of the DNA damage or the induction of apoptosis. Disturbances in these mechanisms can result in an accumulation of DNA alterations that predispose the damaged cells to malignant transformation.

Since 1991, *ATM* has been discussed as a susceptibility gene for breast cancer (Swift et al. 1991), in particular a missense mutation located in the C-terminal third of the ATM protein (c.7271T>G, p.Val2424Gly). For this missense variation a dominant-negative mechanism is described in the literature and in 2006 Waddell used expression profiles to discriminate c.7271T>G carriers from healthy controls (Chenevix-Trench et al. 2002; Waddell et al. 2006).

Based on these expression profiles and the assumption of a dominant-negative effect for the c.7271T>G substitution, I used proteomics-based approaches to elucidate the cellular reactions upon ionizing radiation of lymphoblastoid cell lines from AT patients carrying different *ATM*-mutations, breast cancer patients heterozygous for c.7271T>G, one AT patient homozygous for c.7271T>G, and healthy controls. Based on available literature and the postulated dominant-negative effect, cell lines harboring the c.7271T>G mutation should react in the same manner as cell lines derived from A-T patients with *bona fide ATM* mutations. Further, it should be possible to distinguish carriers of c.7271T>G by noninvasive methods like protein assay and/or chromosomal break analysis.

1. A differential proteomics-approach 2D-gel electrophoresis was used to investigate the response of the protein network in the nucleus to ionizing radiation.
2. A targeted approach was used to identify impaired pathways and check the phosphorylation status of ATM and downstream targets.

# 4. Material and Methods

## 4.1. Materials

### *4.1.1. Chemicals and Kits*

| **Compound** | **Supplier** |
|---|---|
| 3-[(3-Cholamidopropyl)dimethylammonio]-1-propanesulfonate (CHAPS) | AppliChem, Darmstadt |
| 4-(2-Hydroxyethyl)-1-piperazineethanesulfonic acid (HEPES) | Sigma-Aldrich Chemie GmbH, Munich |
| Acetic acid | Sigma-Aldrich Chemie GmbH, Munich |
| Acetone | Sigma-Aldrich Chemie GmbH, Munich |
| Amido Black | Sigma-Aldrich Chemie GmbH, Munich |
| Ammonium acetate | Sigma-Aldrich Chemie GmbH, Munich |
| Annexin V-FITC Kit | Beckman Coulter, Krefeld |
| Bromophenol blue | GE Healthcare Europe GmbH, Freiburg |
| Colcemid | Sigma-Aldrich Chemie GmbH, Munich |
| Coulter Clenz | Beckman Coulter, Krefeld |
| Dithiothreitol (DTT) | Sigma-Aldrich Chemie GmbH, Munich |
| Dulbecco´s PBS (1x) without Mg and Ca, sterile | PAA, Pasching (Austria) |
| Ethylenediaminetetraacetic acid (EDTA) | Carl Roth GmbH + Co KG, Karlsruhe |
| ELISA Kit for NFκB (p65) | Rockland Immunochemicals Inc. |
| Fetal Bovine Serum Gold (FBS) EU-approved | PAA, Pasching (Austria) |
| Giemsa | Carl Roth GmbH + Co KG, Karlsruhe |
| IsoFlow Sheath Fluid | Beckman Coulter, Krefeld |
| L-Glutamine, liquid, 200 mM | PAA, Pasching (Austria) |
| Magnesium chloride ($MgCl_2$) | Sigma-Aldrich Chemie GmbH, Munich |
| Methanol | VWR International GmbH, Darmstadt |
| NP 40 | Biochemica UK Ltd, Billingham, UK |
| p65 ELISA Kit | Rockland Immunochemicals Inc. |
| Phenylmethylsulfonyl fluoride (PMSF) | Sigma-Aldrich Chemie GmbH, Munich |

| | |
|---|---|
| Phenol | Sigma-Aldrich Chemie GmbH, Munich |
| Phosphatase Inhibitor | Sigma-Aldrich Chemie GmbH, Munich |
| Potassium chloride (KCl) | Merck KGaA, Darmstadt |
| Propidium iodide | Fluka, Buchs, Switzerland |
| Proteinase Inhibitor | Sigma-Aldrich Chemie GmbH, Munich |
| RNase A | AppliChem GmbH, Darmstadt |
| RPMI-1640 without L-glutamine | PAA, Pasching (Austria) |
| Sodium chloride (NaCl) | Sigma-Aldrich Chemie GmbH, Munich |
| Sodium dodecyl sulfate (SDS) | Carl Roth GmbH + Co KG, Karlsruhe |
| Sucrose | Sigma-Aldrich Chemie GmbH, Munich |
| Thiourea | GE Healthcare Europe GmbH, Freiburg |
| Trichloroacetic acid (TCA) | Sigma-Aldrich Chemie GmbH, Munich |
| Tris(hydroxymethyl)aminomethane (Tris) | USB Corporation, Cleveland (USA) |
| Tris-HCl | Carl Roth GmbH + Co KG, Karlsruhe |
| Urea | GE Healthcare Europe GmbH, Freiburg |

**Table 1: Chemicals and Kits**

### *4.1.2. Buffers*

| **Name** | **Composition** |
|---|---|
| Bromophenol blue solution 1% | 50 mM Tris<br>1% (w/v) Bromphenol blue |
| Buffer A | 50 mM $NH_4HCO_3$ in aqua dest. |
| Buffer B | 25 mM $NH_4HCO_3$ in 50% acetonitrile |
| Buffer N | 10 mM Tris-HCl, pH 7.4<br>150 mM NaCl<br>1 mM EDTA<br>0.5% (v/v) Triton X-100<br><br>Adding fresh before use: |

| | |
|---|---|
| | 0.5 mM DTT<br>0.5 mM PMSF<br>Proteinase Inhibitor<br>Phosphatase Inhibitor |
| Coomassie staining solution | 34% (v/v) Methanol<br>2% (v/v) Phosphoric acid (98%)<br>17% (w/v) Ammonium sulfate<br>0.066% (w/v) Coomassie G-250 |
| Dense SDS-Buffer | 30% Sucrose<br>2% SDS<br>0.1 M Tris-HCl, pH 8.0<br>5% 2-Mercaptoethanol |
| Equilibration Buffer | 50 mM Tris-HCl, pH 8.8<br>30% Glycerol (99.9%)<br>6 M Urea<br>0.002% (w/v) Bromophenol blue<br>2% SDS |
| Fixation Buffer | Methanol : Acetic acid 3:1 |
| Hypotonic Buffer N | 10 mM HEPES, pH 7.5<br>2 mM $MgCl_2$<br>25 mM KCl<br>Adding fresh before use:<br>1 mM DTT<br>1 mM PMSF<br>Proteinase Inhibitor Cocktail<br>Phosphatase Inhibitor Cocktail |
| L-Buffer | 7 M Urea<br>2 M Thiourea<br>2% (w/v) CHAPS |

| | |
|---|---|
| | 30 mM Tris |
| Nuclear Extraction Buffer A | 10 mM HEPES, pH 7.6<br>15 mM KCl<br>2 mM $MgCl_2$<br>0.1 mM EDTA<br><br>Adding fresh before use:<br>1 mM DTT<br>0.5 mM PMSF<br>Proteinase Inhibitor Cocktail<br>Phosphatase Inhibitor Cocktail |
| Nuclear Extraction Buffer B | Mixing fresh before use:<br>Buffer A + 0.2% NP 40 |
| Nuclear Extraction Sucrose Buffer | Mixing fresh before use:<br>Buffer A + 0.25 M Sucrose |
| Rehydration Buffer | 7 M Urea<br>2 M Thiourea<br>2% CHAPS<br>50 µl Bromphenol blue solution 1% |
| Solution A | 70% Acetic acid |
| Solution B | Methanol: Acetic acid 8:1 |
| Solvent A | 0.1% Formic acid |
| Solvent B | 0.1% Formic acid in acetonitrile |
| TBS-T (10x) | 100 mM Tris<br>150 mM NaCl<br>0.5% Tween20 |

**Table 2: Buffers**

### *4.1.3. Antibodies*

| Antigen | Company | Catalog No | Host | Dilution |
|---|---|---|---|---|
| ATM | Santa Cruz Biotechnology, Inc. | Sc-53173 | Mouse | 1:500 |
| ATM | Acris Antibodies GmbH | SP1131 | Rabbit | 1:1,000 |
| Calreticulin | Calbiochem® | 208912 | Mouse | 1:5,000 |
| Cytochrom C | Santa Cruz Biotechnology, Inc. | sc-7159 | Rabbit | 1:300 |
| GADD45A | Abcam® | Ab76664 | Rabbit | 1:1,000 |
| IKKγ | Abcam® | ab13917 | Mouse | 1:500 |
| Lamin A | Santa Cruz Biotechnology, Inc. | sc-20680 | Rabbit | 1:1,000 |
| Mre11 | Cell Signaling Technology® | #4895 | Rabbit | 1:1,000 |
| p53 | Santa Cruz Biotechnology, Inc. | sc-126 | Mouse | 1:500 |
| p21 | Abcam® | ab16767 | Mouse | 1:1,000 |
| PGK1/2 | Santa Cruz Biotechnology, Inc. | sc-48342 | Mouse | 1:5,000 |
| phospho-ATM (S1981) | Santa Cruz Biotechnology, Inc. | sc-47739 | Mouse | 1:500 |
| phospho-ATM (S1981) | Abcam® | ab81292 | Rabbit | 1:1,000 |
| phospho-CREB (S121) | Novus Biologicals® | NB100-410 | Rabbit | 1:1,000 |
| phosphor-H2AX (S139) | Acris Antibodies GmbH | AP20846PU-N | Rabbit | 1:1,000 |
| phospho-IKKγ (Ser85) | Abcam® | ab63551 | Rabbit | 1:500 |
| phospho-NBS1 (S343) | Acris Antibodies GmbH | AP02356PU-N | Rabbit | 1:1,000 |
| phospho-p53 (Ser15) | Santa Cruz Biotechnology, Inc. | sc-101762 | Rabbit | 1:1,000 |
| phospho-SMC1 (S966) | Bethyl Laboratories Inc. | A300-050A | Rabbit | 1:1,000 |
| phospho-(Ser/Thr) ATM/ATR Substrate | Cell Signaling Technology® | #2851 | Rabbit | 1:2,500 |
| Rad23B | ProteinTech | 12121-1-AP | Rabbit | 1:1,000 |
| SMC1 | Bethyl Laboratories. Inc | A300-055A | Rabbit | 1:1,000 |

**Table 3: Antibodies**

### *4.1.4. Euipment and Consumables*

| **Device** | **Supplier** |
|---|---|
| Autoklav Systec VX-55 | Systec, Wettenberg, Germany |
| Bandelin Sonorex® ultrasonic bath | Bandelin electronic GmbH & Co KG, Berlin, Germany |
| BD FACSCalibur™ | BD Biosciences, Singapore |
| CASY®TT Cell Counter + Analyzer | Roche |
| Cellstar® Cell culture flasks | Greiner Bio-One, Frickenhausen, Germany |
| Concentrator 5301 | Eppendorf, Hamburg, Germany |
| Coulter® Epics® XL-MCL | Beckmann Coulter, Krefeld, Germany |
| Ettan™Dalt six Large Vertical System | GE Healthcare Europe, Munich, Germany |
| Ettan™IPGphor™3 IEF System | GE Healthcare Europe, Munich, Germany |
| Glass slides | |
| Heraeus® HERAcell 240 $CO_2$ Incubator | Thermo Fisher Scientific, Schwerte, Germany |
| Heraeus® HERAsafe HS | Thermo Fisher Scientific, Schwerte, Germany |
| IBL-437 C | Compagnie ORIS Industrie, Gif s/Yvette, France |
| QStar XL MS/MS System | Applied Biosystems, Darmstadt, Germany |
| TripleTOF 5600+ QTOF-mass spectrometer | Sciex, Framingham (USA) |
| VersaDoc MP4000 | BioRad, Hercules, CA, USA |
| Wilovert S inverse Microscopy | Helmut Hund, Wetzlar, Germany |

**Table 4: Equipment and Consumables**

### *4.1.5. Software*

| **Program** | **Supplier** |
|---|---|
| Coulter Expo 32 | Beckman Coulter |
| Image Lab | BioRad, Hercules, CA, USA |
| Mascot 2.2 | Matrixscience, London (UK) |
| MultiCycle AV for Windows | Phoenix Flow Systems |
| PeakView 2.2 | Sciex, Framingham (USA) |
| Progenesis Same Spots | Nonlinear Dynamics |
| Protein Pilot 4.5 | Sciex, Framingham (USA) |
| Quantity One | BioRad, Hercules, CA, USA |
| Analyst 1.7TF | Sciex, Framingham (USA) |

**Table 5: Software**

## 4.2. Cell Culture

### *4.2.1. Cell lines*

EBV-transfected lymphoblastoid cell lines were obtained from Coriell Cell Repositories (CCR) at the Coriell Institute for Medical Research, Camden, NJ, USA (CEPH French Pedigree and Ataxia Telangiectasia Patients) and from the Kathleen Cuningham Foundation Consortium for Research into Familial Breast Cancer, (kConFab) (Breast Cancer Patients with 7271T>G mutation).

| **Name** | **Description** |
|---|---|
| GM12548 | Caucasian; CEPH French Pedigree |
| GM12561 | Caucasian; CEPH French Pedigree |
| GM12672 | Caucasian; CEPH French Pedigree |
| GM12699 | Caucasian; CEPH French Pedigree |
| GM08436 | Caucasian; Ataxia Telangiectasia<br>Paternal allele: 4642delGATA; D1548fsX<br>Maternal allele: 5932G>T; skipping Ex42; E1978X |
| GM09587 | Caucasian, Ataxia Telangiectasia<br>Paternal allele: 9022C>T; 735C>T<br>Maternal allele: 4bp-del IVS59+1 |
| GM13762 | Caucasian, Ataxia Telangiectasia<br>Paternal allele: 8565TG>AA<br>Maternal allele: 6997insA; truncated protein |
| GM13805 | Caucasian, Ataxia Telangiectasia<br>Paternal allele: 6736del20ins2; protein truncation<br>Maternal allele: 1229T>C |
| 98.004.0011 | Caucasian, Breast Cancer Patient<br>(Heterozygous: 7271T>G) |
| 98.004.0012 | Caucasian, Breast Cancer Patient<br>(Heterozygous: 7271T>G) |
| 98.004.0034 | Caucasian, Breast Cancer Patient<br>(Heterozygous: 7271T>G) |

| | |
|---|---|
| 03.005.1294 | Caucasian, Breast Cancer Patient<br>(Heterozygous: 7271T>G) |
| 109 II-6 | Caucasian, Ataxia Telangiectasia<br>(Homozygous: 7271T>G) |

**Table 6: Cell lines used in this study**

### *4.2.2. Cell Culture Conditions and Irradiation Treatment*

All cell lines were cultured with RPMI1640 containing 15% non-heat inactivated fetal bovine serum and 2 mM L-glutamine in a humidified incubator at 37°C in 5% $CO_2$ in culture flasks (25cm$^2$ or 75 cm$^2$) with filter cap. Media was changed 24 hours before treatment and cells were seeded at a final concentration of 1.5 x $10^6$ cells/mL. All cell lines were irradiated with 3 Gy or mock-irradiated using an IBL-437 C (Cesium-137 gamma radiation) blood irradiator and incubated afterwards for 6 hours in the incubator.

## 4.3. Flow Cytometry

### *4.3.1. Annexin-PI-Staining*

Flow cytometry was done to check the viability of the cells after irradiation/mock-irradiation. Therefore, the annexin V – propidium iodide staining kit from Beckmann Coulter was used according to the manufacturer´s protocol.
After treatment and incubation, 2 x $10^6$ cells were collected and centrifuged at 150 x g for 8 min at 8°C. The resulting pellet was resuspended in 100 µL of 1x binding buffer and 1 µL of annexin-FITC and 5 µL of propidium iodide staining solution were added. After incubation for 15 min on ice, 400 µL of 1x binding buffer were added and samples were measured immediately on a Coulter® Epics® XL-MCL Expo 32.

For subsequent sample preparation only cell cultures with a viability ≥ 90% were used.

### *4.3.2. Propidium Iodide (PI)-Staining*

The PI-staining for cell cycle analysis was done in cooperation with Dr. Michael Gruber (Department of Anesthesiology, University Hospital Regensburg, Regensburg, Germany).

For cell cycle analysis, 1 x $10^6$ cells were washed twice with ice-cold PBS/5 mM EDTA and centrifuged at 2,000 x g for 5 min at 4 °C, followed by a fixation step with 100% ethanol and an incubation time of 30 min at room temperature. After centrifugation at 2,000 x g for 5 min at 4 °C, 20 µL of RNase A were added and the suspension was incubated at room temperature for 30 min. Finally, staining with 5 µL propidium iodide (100 µg/mL) was carried out followed by sample analysis on a BD FACSCaliburTM.

## 4.4. Chromosomal Break Analysis

Chromosomal break analysis was done in cooperation with the Center of Human Genetics (Praxis und Labor für Humangenetik Hehr, Regensburg, Germany; Prof. Dr. U. Hehr).

After irradiation/mock-irradiation, colcemid was added to the cells (final concentration 10 µg/ml) incubated for 30 min at 37 °C in 5% $CO_2$. Afterwards, cells were centrifuged at 150 x g at 8°C for 8 min, resuspended in 0.4% pre-warmed KCl and incubated for 10 min at room temperature. Next, the cells were resuspended and washed three times with ice cold Fixation Buffer (methanol: acetic acid 3:1) and finally stored at -20 °C.

To separate metaphases, the suspensions were dropped on ice cold glass slides, dried at 50 °C overnight and stained with Giemsa. The metaphases were captured and chromosomal breaks were counted.

## 4.5. Enzyme-Linked Immunosorbent Assay (ELISA)

To determine the activity of NFκB (p65) in nuclear lysates of irradiated and mock-irradiated cells 6 hours after irradiation, an ELISA Kit (Rockland Immunochemicals Inc.) was used according to the manufacturer's protocol.

A plate - coated with the ds-DNA sequence containing the NF-κB response element - was incubated at 4 °C overnight with 10 µg of nuclear lysate. After washing, the plate was incubated with the first antibody for one hour at room temperature and after an additional washing step the secondary antibody was applied. After a third washing step a developing reagent was added and the absorbance was measured at 450 nm by a photometer.

## 4.6. Nuclei Extraction

After irradiation and incubation, $10^8$ cells were harvested, centrifuged at 150 x g and 8 min at 8 °C and washed three times with ice-cold PBS. For nuclei extraction, all steps were carried out on ice.

### *4.6.1. Nuclei Extraction adapted from Collas et al., 1998 (Collas P.)*

The cell pellets were resuspended in 10 volumes of ice-cold hypotonic buffer N and transferred to a 2.0-mL reaction tube. The cells were chilled on ice for 30 min and homogenized with a glass Dounce pestle. After cell lysis, 125 µL of 2 M sucrose solution per mL cell lysate were added and mixed by inversion. After centrifugation at 150 x g and 8 °C for 8 min and an additional washing step with ice-cold hypotonic buffer N, the supernatant (cytosolic fraction) as well as the pellet (nuclear fraction) were stored a -80 °C.

### *4.6.2. Nuclei Extraction adapted from Hoppe-Seyler et al., 1991 (Hoppe-Seyler et al. 1991)*

The pellet was resuspended in 750 µL of buffer N, transferred to a 2.0-mL reaction tube and left on ice for 5 min. After centrifugation at 1,250 x g and 8 °C for 5 min the supernatant (cytosolic fraction) and the pellet (nuclear fraction) were stored at -80 °C.

### *4.6.3. Nuclei Extraction adapted from Rascle et al., 2003 (Rascle et al. 2003)*

After washing with PBS, the cell pellet was resuspended in 1 mL buffer A and transferred to a 2.0-mL reaction tube. The cells were centrifuged at 850 x g and 4 °C for 1 min and gently resuspended in 1.2 mL buffer B. After centrifugation at 350 x g and 4 °C for 1 min the supernatant (cytosolic fraction) was kept and the pellet (nuclear fraction) was washed with 0.5 mL sucrose buffer, centrifuged and washed again with 0.5 mL buffer A. Afterwards, the nuclear and cytosolic fractions were stored at -80 °C.

## 4.7. Protein Precipitation

After sample preparation the proteins of the cytosolic fraction were precipitated with 100% ice-cold ethanol at -20 °C overnight. Afterwards the pellet was air dried and dissolved in L-buffer.

The proteins of the nuclear fraction were precipitated according to the protocol of Wang et al., 2003 (Wang et al. 2003). First, the pellet was resuspended in 10% TCA/acetone and centrifuged at 14,000 x g and 4 °C for 3 min. This was followed by a first washing step with ice-cold 80% methanol / 0.1 M ammonium acetate and a second washing step with 80% ice-cold acetone. Afterwards, the proteins were extracted using a 1:1 mixture of phenol and dense SDS-buffer, pH 8.0. This mixture was centrifuged at 16,000 x g and 4 °C for 3 min to separate the two phases. The upper phenol phase was transferred in a new 2.0-mL reaction tube, mixed with 5 volumes of ice-cold 80% methanol / 0.1 M ammonium acetate and stored at -20 °C overnight. After centrifugation at 16,000 x g and 4 °C for 3 min the pellet was washed first with 100% ice-cold methanol and in a second step with 80% ice-cold acetone. Afterwards, the pellet was air dried and dissolved in L-buffer.

## 4.8. Protein Quantification

After protein precipitation the protein content of the cytosolic fraction was determined using the FluoroProfile® Kit according to the manufacturer's protocol.

For the protein quantification of the nuclear fraction a modified protocol from Schaffner and Weissmann, 1973 (Schaffner and Weissmann 1973) was used. The sample was diluted 1:100 with Aqua dest. and 200 µL of solution A were added. After incubation on ice for 10 min the sample was centrifuged at 4,000 x g and 4 °C for 5 min and washed three times with solution

B. Finally, the precipitate was dissolved in 400 µL 1 M NaOH and the absorption was measured with a photometer at 595 nm. To quantify the sample, a BSA standard (0.3 µg to 20 µg) was used.

## 4.9. Immunoblotting

For gel electrophoresis, the nuclear samples were denatured at 96 °C for 10 min. Five µg of protein per lane were loaded on a pre-cast polyacrylamide gel that was run according to the manufacturer's protocol.

To separate proteins with a molecular weight > 150 kDa, the NuPAGE® 3-8% Tris acetate pre-cast polyacrylamide gel system was used. For proteins with a molecular weight between 25 – 150 kDa, the NuPAGE® 4-12% Bis-Tris pre-cast polyacrylamide gel system, and for proteins < 25 kDa Novex® 16% tricine gels were used. After separation, the proteins were blotted on a PVDF membrane (Immobilon-P or Immobilon-PSQ for proteins < 25 kDa). The protein transfer was carried out in an XCell SureLock® Blot Module with 25 V at 4 °C according to the manufacturer's protocol.

To transfer proteins with a molecular weight >150 kDa and < 25 kDa the following transfer buffers were used:

| | |
|---|---|
| 800 mL | Aqua dest |
| 150 mL | Methanol |
| 50 mL | 20 x NuPAGE ®Transfer buffer |

**Table 7: Transfer Buffer 1**

For proteins with a molecular weight range from 25 – 150 kDa the following transfer buffer was used:

| | |
|---|---|
| 850 mL | Aqua dest |
| 100 mL | Methanol |
| 50 mL | 20 x NuPAGE ®Transfer buffer |

**Table 8: Transfer Buffer 2**

The successful protein transfer was controlled by Ponceau red staining and afterwards the membrane was incubated with Roti®Block at 4 °C overnight. The PVDF membrane was washed three times with 1 x TBS-T and incubated with the first antibody (diluted in 1x TBS-T). The required concentration was checked before with a test experiment. After three additional washing steps the second antibody was applied diluted in 1x TBS-T. This was followed by three

subsequent washing steps with 1 x TBS-T and afterwards the immunopositive bands were visualized by using Amersham ECL PlusTM Western Blotting Detection Reagent as directed by the manufacturer. Equal protein loading was monitored by staining an identically loaded gel with Coomassie Brillant Blue.

## 4.10. 2D-Gel Electrophoresis

### *4.10.1. Isoelectric Focusing (1st Dimension)*

For the analysis of the nuclear proteome of the irradiated and non-irradiated cells, two different pH gradients were used.

The nuclear samples were separated either on ImmobilineTM DryStrips Gels pH 3 – 10 (nonlinear), 24 cm, or on SERVA IPG BlueStrips pH 3 - 10; 24 cm. In contrast, the cytosolic proteins were run on SERVA IPG BlueStrips pH 4 - 7; 24 cm.

The strips were rehydrated overnight with rehydration buffer and the samples were applied via cup-loading at the acidic end of the IPG strip. Isoelectric focusing was carried out in an EttanTM IPGphorTM 3 IEF System with the following settings.

| **Step and Voltage method** | **Voltage (V)** | **Time (h:min)** | **Vhrs** |
|---|---|---|---|
| Step´n´Hold | 150 | 2:00 | 300 |
| Step´n´Hold | 300 | 2:00 | 600 |
| Gradient | 500 | 2:00 | 800 |
| Gradient | 1000 | 4:00 | 2250 |
| Gradient | 4000 | 3:00 | 7500 |
| Gradient | 6000 | 0:30 | 2500 |
| Step´n´Hold | 6000 | 6:30 | 39000 |
| | | ∑ 19:00 | ∑ ~53000 |

**Table 9: IEF settings**

After the IEF, the strips were equilibrated for 20 min in equilibration buffer supplemented with 1% (w/v) DTT for reduction of cystine. In a second equilibration step, the strips were incubated for 20 min with equilibration buffer containing 2.5% (w/v) iodoacetamide for alkylation of SH-groups.

### *4.10.2. SDS-Polyacrylamide Gel Electrophoresis (2nd Dimension)*

For the second dimension either vertical or horizontal electrophoresis was used.

**Vertical 2nd Dimension**

After the first dimension the IPG strips were sealed with 0.5% agarose in SDS running buffer on top of 12.5% acrylamide gels. The SDS-PAGE step was performed on an Ettan™ Dalt six Large Vertical System at 5 W per gel for 0.5 h followed by a 4.5 h step with 20 W per gel.

**Horizontal 2nd Dimension**

The IPG strips were applied on a 2D HPETM Large Gel NF 12.5% and run on a HPETM Tower System at 1 W per gel. After 30 min, the strip was removed and the second electrophoresis was continued at 30 W per gel for 3.5 h.

## 4.11. In-Gel-Protein Detection

### *4.11.1. Pre-Staining with CHROMIS 3x DGE – Minimal Labeling Kit (for the nuclear proteome 6 hours after irradiation)*

To study the differences between the irradiated and non-irradiated nuclear proteomes the samples were labeled with fluorescent CHROMIS Dyes (Cyanagen).

Briefly, 50 µg each of nuclear extract from the irradiated and non-irradiated cells and a mixture of 25 µg from each as internal standard were labeled with different fluorescent dyes according to the manufacturer's protocol. The three samples were combined and loaded via cup loading on an IPG strip. After 2D electrophoresis, the spots on the gels were visualized by the FLA-5000 Imaging system and analyzed using the Progenesis SameSpots software.

### *4.11.2. LavaPurple™ (for the nuclear proteome 1 hour after irradiation and for the cytosolic proteome 6 hours after irradiation)*

To compare the nuclear proteome 1 hour after treatment as well as the cytosolic proteome 6 hours after treatment, the LavaPurple™ fluorescent staining kit was used. The irradiated and non-irradiated samples were run in a single experiment on separate 2D gels, which were stained according to the manufacturer's protocol. Afterwards, the spots on the gels were visualized using the VersaDoc™ MP4000 Imaging System and analyzed with the Progenesis SameSpots software.

### *4.11.3. Coomassie G-250 according to Neuhoff et al., 1988 (Neuhoff et al. 1988)*

Coomassie G-250 staining was used for protein visualization and subsequent spot picking. Therefore, the gels were incubated overnight at 4 °C in the Coomassie staining solution. The gels were destained the next day with Aqua dest. to remove background staining and visualized using the VersaDoc™ MP4000 Imaging System.

### *4.11.4. Silver Staining according to Blum et. al., 1987 (Blum et al. 1987)*

For mass spectrometry-based identification of protein spots, the gels were post-stained with a modified silver staining protocol from Blum et al., 1987 (Blum et al. 1987).

| Task | Chemicals | Duration |
|---|---|---|
| Fixation | 40% (v/v) Ethanol<br>10% (v/v) Acetic acid | Overnight at 4°C |
| Washing | 30% (v/v) Ethanol | 2 x 20 min |
| Washing | Water | 1 x 20 min |
| Sensitizing | 0.02% (w/v) Sodium thiosulfate | 1 min |
| Washing | Water | 3 x 20 sec |
| Staining | 0.1% (w/v) Silver nitrate | 20 min at 4°C |
| Washing | Water | 3 x 20 min |
| Developing | 3% (w/v) Sodium carbonate<br>0.05% (v/v) Formaldehyde | Developing time depends on the intensity of the spots |
| Stop | 0.05 M (w/v) EDTA | 20 min |

**Table 10: Silver staining protocol**

### *4.11.5. Image Analysis*

After separation in the second dimension, gels were visualized using the VersaDocTM MP 4000 Imaging System or the FLA 5000 Imaging System. Afterwards, the images were cropped and imported into the Progenesis SameSpots Software as linear tif-files. First a quality control was done, followed by an image alignment and automatic analysis with background subtraction and normalization. To compare the gels with each other, a 'within-subject design' was used and an ANOVA was carried out. Only spots with a $p$-value ≤ 0.05 and a Power ≥ 0.8 were used for spot picking.

## 4.12. Protein Identification with Mass Spectrometry

### *4.12.1. In-Gel-Digestion using Trypsin*

After separation in the first and second dimension the gels were analyzed using the Progenesis SameSpots software. Gels chosen for picking were stained with silver staining or Coomassie G250 and the selected spots of interest were excised. Afterwards the 2D-Spots were washed in an alternated way for 10 min in buffer A and 10 min in buffer B. After washing the spots

were dried in a vacuum centrifuge, then digested with trypsin (12.5 ng/µL) overnight at 37 °C and extracted using 5% formic acid.

### *4.12.2. Nano-LC-MS/MS*

For pre-column concentration, 15 µL of the protein digests were applied by sandwich injection onto an Acclaim PepMap 300 C18 pre-column (end-capped, 5 mm x 0.3 mm ID, 3 µm particle size, 300 Å pore size, flow rate 10 µL/min) using solvent A operated on a nano-HPLC (Ultimate 3000, Dionex). Afterwards, the peptides were separated by reversed phase liquid chromatography (Acclaim PepMap100 C18; end-capped, 150 mm x 75 µm ID, 3 µm particle size, 100 Å pore size) with a 36-min binary gradient from 4 – 40 % solvent B and a flow rate of 300 nL/min. The nano-HPLC was directly coupled to a QStar XL qTOF mass spectrometer equipped with a nano-ESI source. Repeated full scan MS spectra (from m/z 400 – 1.200) were acquired for 1 s, followed by two MS/MS scans of the two most intensive precursor ions for 2.5 s. Every ion selected for fragmentation was excluded for 30 s by dynamic exclusion and the trigger threshold was set to 20 counts.

### *4.12.3. Data Analysis using Mascot*

All acquired spectra were processed using Mascot 2.2 and database searches were performed against the SwissProt human database (last modified 05.2011). Carbamidomethylation, Gln-pyroGlu (N-term Q) modification and Oxidation (M) were selected as fixed modifications. A peptide tolerance of ± 0.2 Da and MS/MS tolerance of ± 0.2 Da were allowed and the number of maximum missed cleavages was set to 1. Proteins that were identified by at least 2 unique peptides were taken into account and if more than one protein per spot was identified, the exponentially modified protein abundance index (emPAI) was consulted for decision.

### *4.12.4. SWATH-MS-based analysis of nuclear extracts*

Hundred µg of uclear protein lysate were used for filter-aided sample preparation (Wisniewski et al. 2009) and aliquots of 1 µg were used for acquisition of the SWATH-MS runs (Gillet et al. 2012). For generation of the protein library, six runs were performed using 1 µg. For each run one group (controls with/without irradiation; breast cancer patients with/without irradiation and A-T patients (including 109II-6) with/without irradiation) were pooled, respectively. The information-dependent acquisition (IDA)-runs for library generation were accomplished on a TripleTOF 5600+ mass spectrometer (ABSciex, Darmstadt, Germany) coupled online to a Dionex Ultimate3000 nano-HPLC (ThermoFisher, Dreieich, Germany). Nano-HPLC analysis was conducted using peptide trapping (Acclaim PepMap, 2 cm length x 200 µm I.D., 3 µm particle size, flow rate 5 µL/min, 0.1% formic acid at 35 °C) and a 88-min binary gradient (4-30% B in 73 min, 30-45% B in 15 min) on a 25 cm Acclaim PepMap column (75 µm I.D., 3 µm particle size, flow rate 250 nL/min at 35 °C). The mass spectrometer was operated in IDA-mode with a TOF-MS from 400-1000 m/z for 250 ms followed by MS/MS-spectra from 230-1500 m/z of the 30 most intensive precursor ions for 100 ms per precursor. The data was searched using ProteinPilot 4.5 (ABSciex) against the Uniprot-database with the following adjustments: sample type “Identification”, Cys alkylation “Iodoacetamide”, digestion “Trypsin”, taxonomy

“Homo sapiens”, search effort “RapidID”, detected protein threshold “0.05 (10%)” with false discovery rate (FDR) analysis. The result file was used for generation of the libraries of 1,700 proteins identified with an FDR of 1% by PeakView 2.1 (ABSciex) using only spectra with a confidence of 95% or higher of unique, unmodified peptides with up to 6 peptides per protein and 6 transitions per peptide.

Nano-HPLC separation for the SWATH-MS analyses was accomplished using the same conditions as in the IDA-run. The typical obtained peak width (base-to-base) was about 30 seconds. Therefore, the TripleTOF 5600+ was operated in SWATH-mode with a fixed duty cycle length of 3.3 s to obtain nine data points per LC peak. After a 50 ms TOF-MS scan, the entire m/z range of 400-1,000 was covered using 43 SWATH-windows of a quadrupole isolation width of 15 m/z, respectively (Simbürger et al. 2016). For all SWATH-analyses the retention times were aligned to the respective library using manually chosen peptides distributed evenly over the chromatographic run. For SWATH-processing, XICs were obtained with an “XIC-width” of 75 ppm and retention time windows of 10 min, respectively. The FDR-threshold was set to 1%.

# 5. Results

## 5.1. Sequencing breast cancer patients

In 2002, Chenevix-Trench *et al.* identified the c.7271T>G variant by an indirect approach using the restriction endonuclease assay, followed by direct Sanger sequencing (Chenevix-Trench et al. 2002). To verify the substitution conventional Sanger sequencing was applied to all lymphoblastoid cell lines of the breast cancer patients. All of them carried the original described missense mutation at position c.7271, which leads to an amino acid change at position 2424 from valine to glycine (Figure 1).

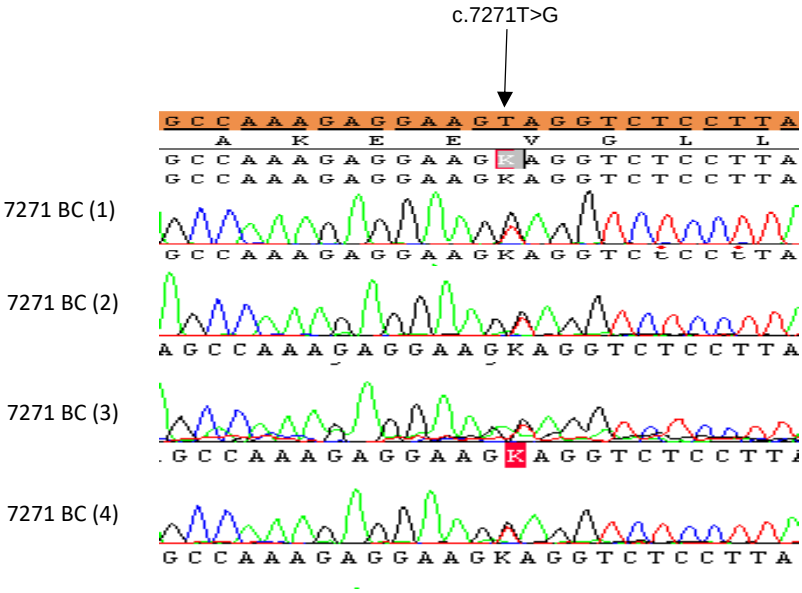


**Figure 1: Sequencing results of the 7271 BC patients; the mutant position is indicated by the arrow; the normal DNA sequence is shown in the upper orange line**

## 5.2. Effect of different *ATM* mutations on cell growth, cell viability and cell death after irradiation with 3 Gy

The irradiation of cells with ionizing radiation leads to DNA damage and subsequent cell cycle arrest for DNA repair. In cell culture, lymphoblastoid cell lines double nearly every 36 hours. Hence, cell count is an easy and fast measure to assess the effect of ionizing radiation on different cell lines. To that end, cells were irradiated with 3 Gy or mock-irradiated, followed by a resting step in the incubator. 42 hours after irradiation, the cell number was measured using a CASY® cell counter (OMNI Life Science). Figure 2 displays cell counts (Mio cells per mL) for the control cell lines, the cell lines derived from the A-T patients, and the breast cancer patients harboring the c.7271T>G variant, respectively. All irradiated cell lines showed a decreased number of cells, which could be due to cell cycle arrest and/or an increase in apoptotic or necrotic cells.

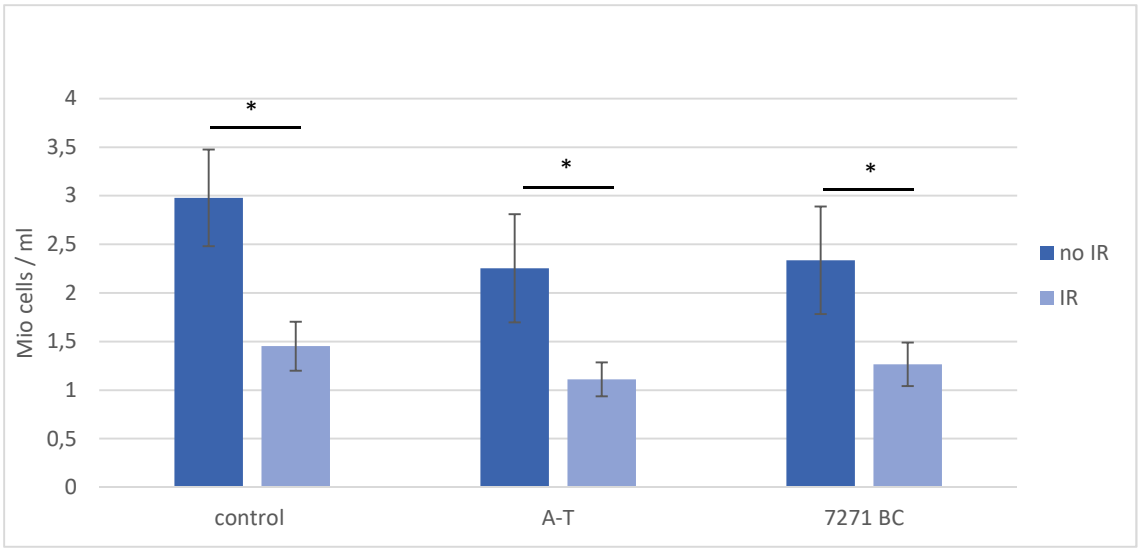


**Figure 2: Cell count for each group (four cell lines per group) measured 42 hrs after irradiation with a CASY cell counter (* p≤0.05, unpaired two-tailed student´s Ttest).**

To further investigate these groups and to differentiate between late apoptotic/necrotic and early apoptotic cells, Annexin-PI staining was carried out, followed by flow cytometry. Flow cytometry was developed in 1968 by W. Göhde from the University of Münster and is used to measure multiple characteristics of individual particles flowing in single file in a stream of fluid (Dittrich und Ghode). Light scattering at different angels can distinguish differences in size and internal complexity. Furthermore, cell components can be labelled with fluorescent dyes to identify a wide range of cell surface or cytoplasmic antigens.

To distinguish viable, apoptotic and necrotic cells after irradiation with 3 Gy vs mock-irradiation, an Annexin-PI staining was carried out. All cell lines were irradiated or mock-irradiated followed by a resting step for 42 hours in the incubator and thereafter labelled with annexin and PI and measured by flow cytometry. Annexin-PI is used widely to determine if cells are viable, apoptotic or necrotic through differences in plasma membrane integrity and permeability (Vermes et al. 1995; Vermes et al. 2000). The ability of PI to enter a cell is dependent upon the permeability of the plasma membrane. Viable or early apoptotic cells have an intact plasma membrane and, therefore, PI cannot enter the cell. Nevertheless, early apoptotic cells can be distinguished from viable cells by annexin staining of phosphatidyl residues on the cell membrane. In viable cells, these residues position on the inside of the plasma membrane, whereas in early apoptotic cells these residues are exposed on the outer surface and, therefore, are accessible to fluorescent labelling with annexin. In late apoptotic or necrotic cells the integrity of the cell membrane as well as the nuclear membrane decreases, PI can pass through the membranes and intercalate with the DNA. Due to the presence of phosphatidyl residues in these necrotic/late apoptotic cells, these cells are double positive for PI and annexin. Figure 3 shows the percentage of viable, late apoptotic/necrotic and early apoptotic cells after irradiation or mock-irradiation for four cell lines in each group. Comparing the viable cells in the three groups without irradiation the percentage is nearly the

same in control cells and in cell lines from breast cancer patients harbouring the heterozygous c.7271T>G mutation (95.09% (controls) and 94.13% (7271)) and slightly decreased in the A-T cell lines (91.13%). However, the amount of early apoptotic cells is much higher in the cells derived from A-T patients compared to the control cell lines and the breast cancer cell lines (4.49% (controls), 4.84% (7271) and 7.2% (A-T)). The late apoptotic/necrotic show a nearly similar trend (0.42% (controls), 1.04% (7271) and 1.67% (A-T)). An irradiation with 3 Gy amplified these effects and lead to an increase from 3.6% in the control cell lines vs 11.56% and 4.27% in the A-T and breast cancer cell lines. In contrast to this the amount of apoptotic cells between the control cell lines and the A-T and breast cancer cell lines, respectively, after irradiation decreased from 7.93% in the controls to 5% and 5.39% in the A-T and c.7271T>G cell lines, respectively.

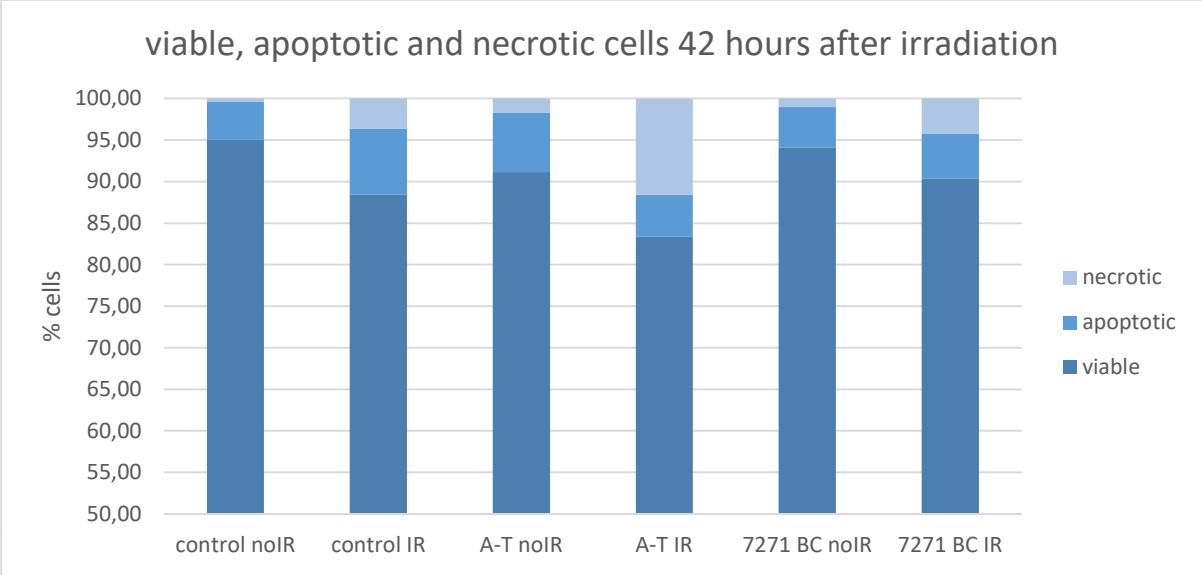


**Figure 3: Percentage of viable, necrotic and apoptotic cells 42 hours after irradiation with 3 Gy measured by A-PI staining using flow cytometry (four cell lines per group)**

## 5.3. Effect of different ATM mutations on cell cycle checkpoints after irradiation with 3 Gy

Irradiation of viable cells with ionizing radiation induces DNA double-strand breaks (DSBs). Generally, cells are able to recognize these breaks before they progress to the next phase of the cell cycle at so-called cell cycle checkpoints. Control mechanisms at these checkpoints ensure that the DNA is intact and that each stage of the cell cycle is completed before the following stage is initiated. If damaged DNA is recognized, the progression through the cell cycle is blocked until the damage is repaired (= cell cycle arrest). Arrest in G1 and S phase prevents copying of damaged bases, which would fix mutations in the genome. An arrest in G2 phase allows the repair of damaged DNA. A PI staining followed by flow cytometry reveals the percentage of cells at each cell cycle stage.

After irradiation with 3 Gy or mock-irradiation, all cells were stained with PI and the percentage of cells in each cell cycle phase was measured by means of a flow cytometer. Figure 4 shows a significant difference (p = 0.008) in the percentage of cells in the G1 Phase between irradiated (33%) and non-irradiated A-T cells (43%), respectively. In contrast, ionizing radiation exerted no impact on the relative numbers of control and c.7271G>T breast cancer cells in the G1 phase. Comparing the effect of irradiation among all three cell lines, a significant difference is shown for the A-T cells compared to the control cells (p = 0.013) and the breast cancer cells ($p = 0.43*10^{-4}$).

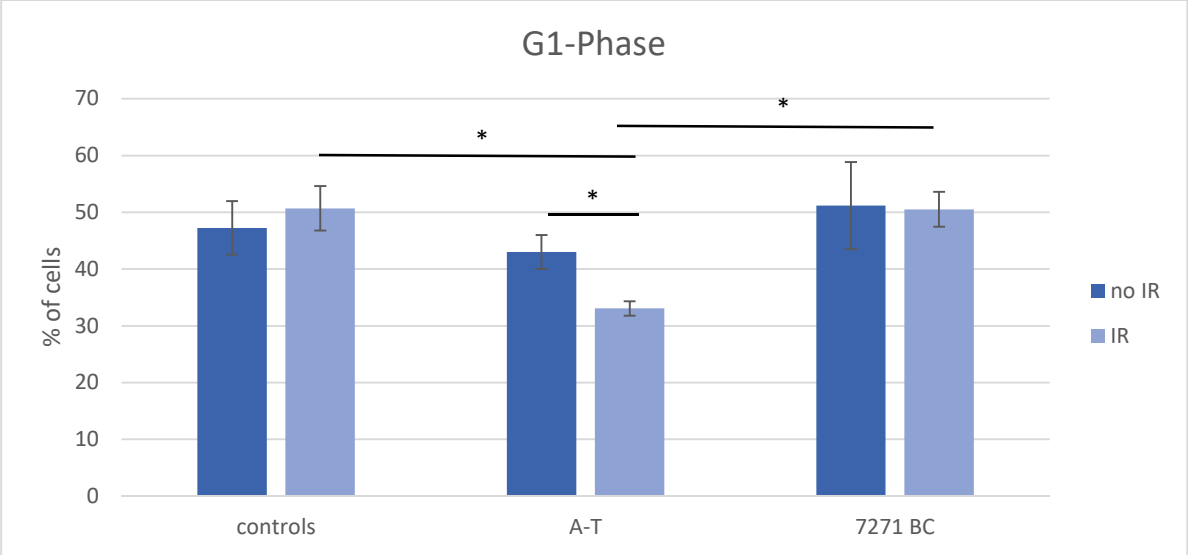


**Figure 4: Percentage of cells arrested in G1 phase after irradiation with 3 Gy (four cell lines per group) (*p≤0.05, (one-way ANOVA with subsequent Tukey´s post hoc T-test))**

In Figure 5 the effect of irradiation in the S phase is depicted. Actually, there is no difference between control cell lines, A-T cell lines and cell lines derived from breast cancer patients with the c.7271T>G variant with or without irradiation. Nevertheless, an intra-group comparison shows a significant difference between irradiation and non-irradiation in the controls and in the cell lines derived from A-T patients. The cell lines derived from breast cancer patients that harbour the heterozygous c.7271T>G variant show the same trend but a higher variance.

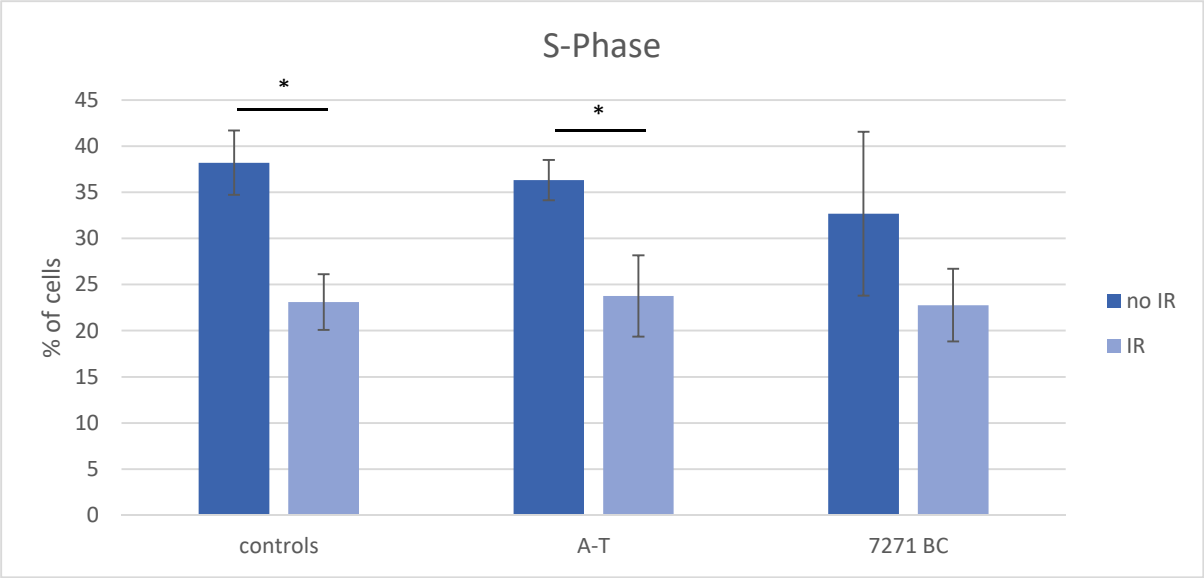


**Figure 5: Percentage of cells arrested in S phase after irradiation with 3 Gy (four cell lines per group) (*p≤0.05) (one-way ANOVA with subsequent Tukey´s post hoc T-test))**

The percentages of cells in the G2-/M-phase are shown in Figure 6. After irradiation, all cell lines show a significant higher percentage of cells in G2-/M-phase compared to the non-irradiated cells. Additionally, the A-T cell lines show a significant higher increase of cells that are arrested in the G2/M phase after irradiation compared to the controls (p = 0.4*10-3) and the c.7271T>G cell lines (p = 0.58*10-3).

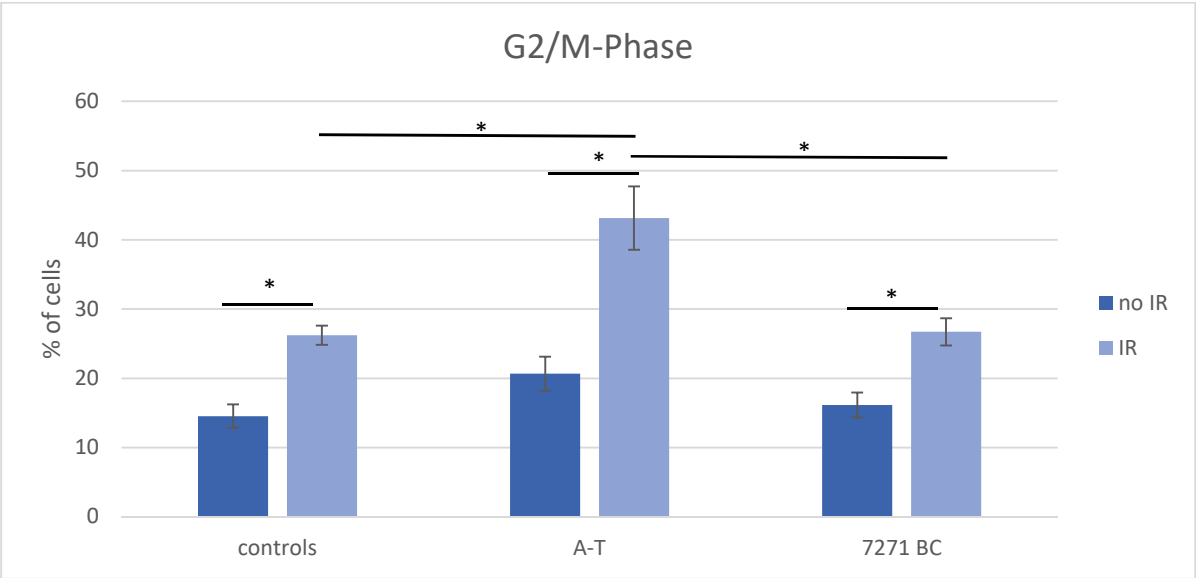


**Figure 6: Percentage of cells arrested in G2/M phase after irradiation with 3 Gy (four cell lines per group) (*p≤0.05, (one-way ANOVA with subsequent Tukey´s post hoc T-test))**

## 5.4. Analysis of chromosomal breaks after irradiation with 3 Gy

Chromosomal breaks are one of the key molecular findings in A-T patients. To measure the chromosomal breaks, a control, an A-T, and a c.7271T>G cell line were irradiated with 3 Gy or

mock-irradiated followed by a resting step in the incubator. Afterwards all cell lines were incubated with colcemid to arrest most of the cells in the metaphase stage and to prevent them from proceeding to the subsequent anaphase stage. After fixation the cells were dropped on a slide and stained with Giemsa. Metaphases were analysed and all chromosomal breaks were counted. Figure 8 shows an exemplary metaphase from each cell line (control, A-T, and c.7271). Chromosomes show their characteristic banding and chromosomal breaks are highlighted with red circles. For the control cell lines, 26 metaphases were analysed and 20 of them showed no chromosomal breaks. There were five metaphases with only one chromosomal break and one metaphase with two breaks. Thirty-two metaphases were analysed for the cell lines derived from A-T patients. They showed a much higher frequency of chromosomal breaks compared to the controls. Thirteen metaphases had no chromosomal breaks, 10 metaphases showed one break per metaphase, seven metaphases two breaks per metaphase and one metaphase each had three and four breaks per metaphase, respectively. For the cell lines from the breast cancer patients harbouring the c.7271T>G variant, 23 metaphases were analysed. Twelve of them showed no chromosomal breaks, seven had one break per metaphase, three metaphases showed two breaks and one metaphase was found with four chromosomal breaks per metaphase. Therefore, the number of chromosomal breaks per metaphase were higher in the A-T cells and c.7271T>G cells, respectively, compared to the control cell line.

**Figure 7: Exemplary metaphases stained with Giemsa showing chromosomal breaks (indicated by red circles)**

| breaks/metaphase | Control cells | A-T cells | 7271T>G cells |
|---|---|---|---|
| 0 | 20 | 13 | 12 |
| 1 | 5 | 10 | 7 |
| 2 | 1 | 7 | 3 |
| 3 | 0 | 1 | 0 |
| 4 | 0 | 1 | 1 |

**Table 11: Number of analysed metaphases and chromosomal breaks per metaphase in all cell lines**

## 5.5. Comparison of different nuclei enrichment protocols

To further investigate the effect of different mutations in the *ATM* gene upon the cellular response to ionizing radiation, two-dimensional fluorescent gel electrophoresis (DIGE) was carried out. However, whole cell lysate represents a too complex mixture for analysis. Further, the main response machinery for ionizing radiation-induced DNA repair is located in the nucleus. Therefore, a protocol for cell lysis and nuclei enrichment has to be carried out, for which three different protocols were tested, followed by Western Blot analysis to determine the purity of the subcellular compartment. Western blotting, or immunoblotting is commonly used to identify a specific protein of interest using the specificity of the antigen-antibody interaction. This method was introduced by Towbin and colleagues (Towbin et al. 1979).

All three protocols were tested with a control cell line and the subcellular fractions were collected to determine the purity of each fraction by using specific antibodies for proteins common in this subcellular compartment. Lamin A is a component of the nuclear protein complex and different lamins form a two-dimensional network along the inner surface of the inner nuclear membrane. Therefore, Lamin A can be used as a specific antibody for the nuclear fraction. Phosphoglycerate kinase (PGK) is a glycolytic enzyme that catalyses the conversion of 1,3-diphosphoglycerate to 3-phosphoglycerate and ATP. Due to its function in glycolysis this protein is located in the cytoplasm and serves as a marker for the cytoplasmic fraction. The protein calreticulin is located in the endoplasmic reticulum (ER) and binds to misfolded proteins after translation of their mRNA to their amino acid structure. It prevents these proteins from being transported to the Golgi apparatus. Additionally, calreticulin binds together with calnexin to certain N-linked oligosaccharides on growing nascent chains.

All three protocols showed an enrichment of the nuclear fraction. However, the protocol of Collas et al. (Collas P.) shows only a small amount of nuclei enriched in this subcellular fraction and also less cytosol. With the protocol of Hoppe-Seyler (Hoppe-Seyler et al. 1991) the enrichment of nuclei is also insufficient whereas the enrichment of the cytosolic fraction was effective. The best results were obtained with the protocol by Rascle (Rascle et al. 2003). The Western Blot analysis shows a sufficient enrichment of nuclei in the subcellular fraction, which is not contaminated by cytosol. Nevertheless, the purified nuclear fraction contains compartments of the endoplasmatic reticulum (Figure 8). The membranes of the endoplasmic reticulum are connected to the outer nuclear membrane. Therefore a slight contamination of endoplasmic reticulum has to be accepted for intact nuclei.

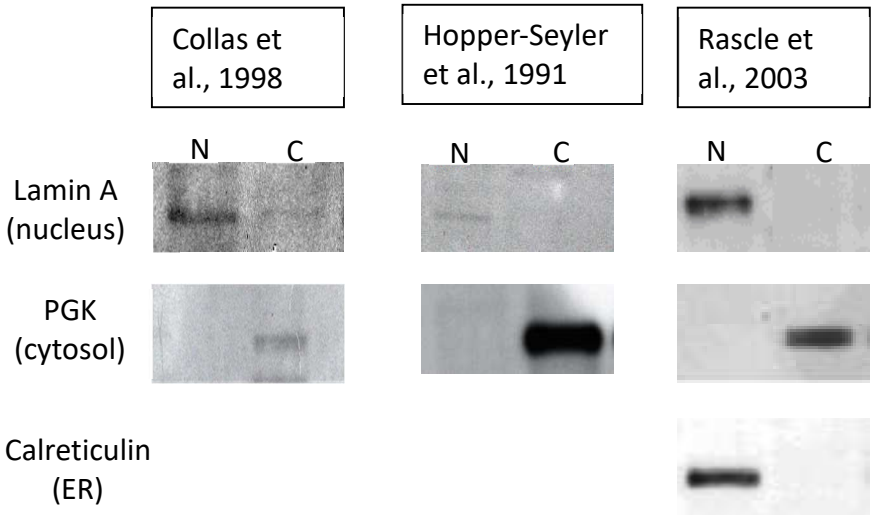


**Figure 8: Western Blot analysis showing the different analyses for each subcellular fraction.**

## 5.6. 2-D Fluorescence Differential Gel Electrophoresis (DIGE) of nuclei enriched fractions

Proteome analysis is a direct measurement of a complex protein network in terms of the presence and relative abundance of different proteins. Therefore, two-dimensional fluorescent gel electrophoresis (DIGE) was carried out using nuclei-enriched fractions. DIGE was first described in 1975 by O'Farrell (O'Farrell 1975).

The general workflow of two-dimensional gel electrophoresis is a two-step process. After sample preparation the first dimension – the isoelectric focusing - is carried out, where the proteins will be separated on the basis of their isoelectric point (PI). The PI is the pH at which a protein carries no net charge and will not migrate in an electric field. After an equilibration step, to reduce disulphide bonds the proteins are separated due to their molecular weight (MW) in the second dimension using SDS gel electrophoresis. The use of different fluorescent dyes allows multiplexing of samples on a 2D gel, shows a good sensitivity and linearity and in combination with computer-assisted image evaluation systems it allows a quantitative and qualitative examination of the proteome.

For this approach all non-irradiated samples were labelled with Cy5, all irradiated samples were labelled with Cy3 and a combination of non-irradiated and irradiated sample was used as a standard mixture and was labelled with Cy2. After the computer-assisted comparison (irradiated vs non-irradiated in each group) all significantly regulated spots were evaluated, followed by silver staining of the gels and the picking of all regulated spots. These spots were washed, destained and analysed by mass spectrometry (Figure 9).

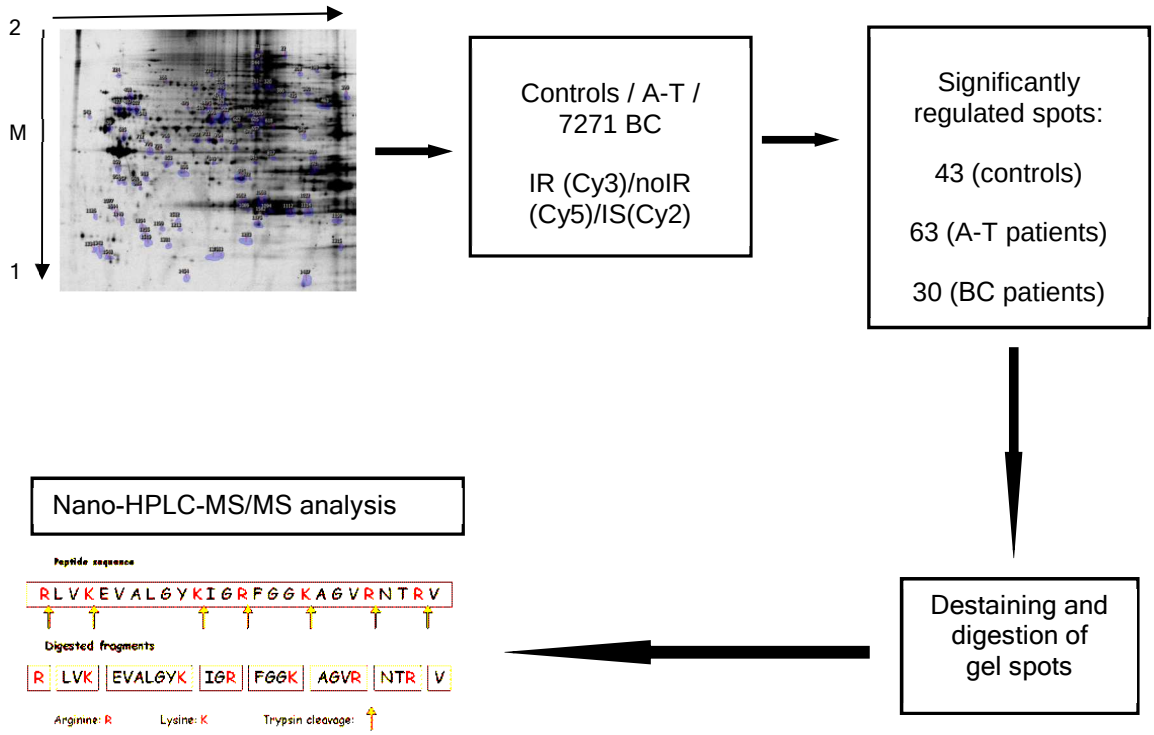


**Figure 9: DIGE Workflow**

In the control cell lines 43 spots were significantly regulated and all spots could be detected on the silver stained gel. Out of these 43 spots 64 proteins could be identified, including 44 nuclear proteins. In the cell lines derived from A-T patients, 63 spots were significantly regulated and picked on the silver gel. 43 proteins were detected – 16 nuclear proteins – in 19 analysed spots. For the cell lines derived from breast cancer patients heterozygous for the c.7271T>G variation 42 significantly regulated spots were evaluated. But only 30 spots could be detected on the silver gel. In 26 spots were 43 proteins detected – 21 nuclear proteins (Fig. 10). Due to low protein concentration it is not possible to detected proteins in every picked spot.

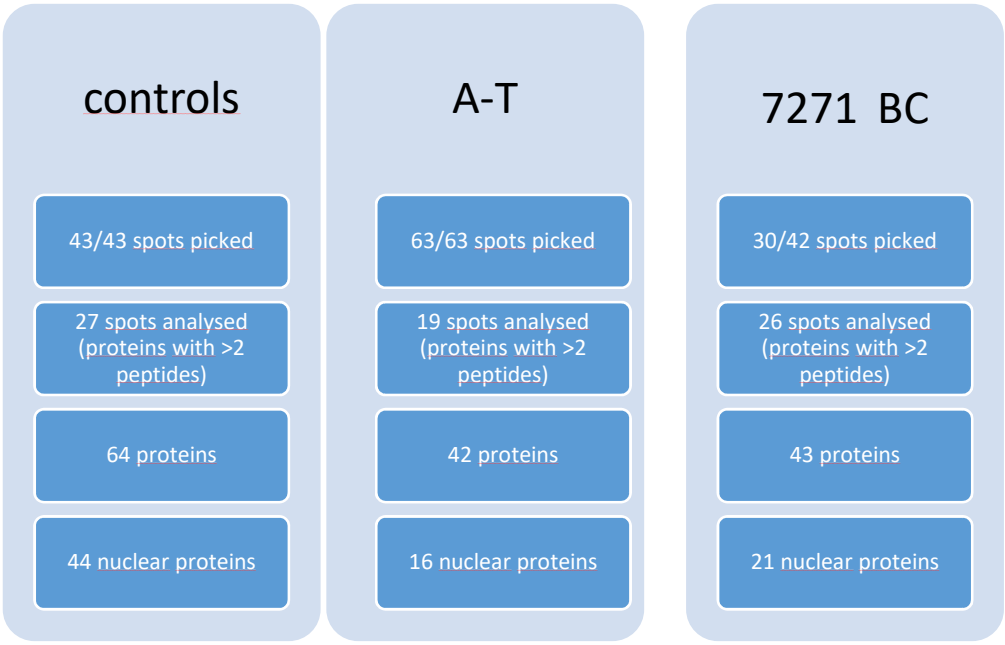


**Figure 10: Overview of detected, picked and analysed DIGE spots**

## 5.7. SWATH analysis

Various so-called „data-independent acquisition“(DIA) methods for quantitative bottom-up proteomics approaches have gained wide popularity through the last years (Hu et al. 2016). These approaches yield more comprehensive data sets and avoid the „missing data problem“ (Roderick J. A. Little, Donald B. Rubin 2002) typically associated with data-dependent approaches and also 2D-PAGE-based analyses. Using the DIA-method „SWATH“(Sequential window acquisition of all theoretical fragment-ion spectra) (Gillet et al. 2012), it was possible to quantify 1,700 proteins over the entire sample set by targeted extraction. Moreover, the methodology allows to re-question the measured data set concerning further, currently not detected proteins by enlarging the used library by future experiments.

SWATH-mass spectrometry is a shotgun proteomic method to quantify proteins. Therefore, protein samples are digested proteolytically into a highly complex peptide mixture prior to LC-MS/MS-measurement. The SWATH-analyses can be divided into two different steps – the library generation and the targeted extraction of quantitative data. For the first step a data-dependent acquisition is used to identify as many peptides/proteins as possible from the proteolytically digested complex sample. Therefore, the mass spectrometer measures throughout the entire LC-gradient repeatedly the following composition: Firstly, the most intensive signals from a Full-MS-scan (e.g. TOP20) are selected for subsequent highly selective isolation and acquisition of respective MS/MS-spectra. In a second step these MS/MS-spectra are used to identify as many peptides as possible by database searches. However, this method is not suitable for quantification due to the high undersampling rate. But it could be used to generate a library of peptide identities, respective retention times and MS/MS-spectra and these data can be used for targeted extraction of MS/MS-signal intensities from subsequent SWATH-runs. During these SWATH-runs the mass spectrometer repeatedly measures MS/MS-

spectra of multiple wide precursor windows (e.g. 25 m/z per window) scanning the entire mass range relevant for shotgun proteomic analyses (e.g. 400-1,250 m/z). As several peptides may be contained within a distinct window and thereby fragmented in parallel, the respective MS/MS-spectra are highly complex and not suitable for identification by database searches. However, the data from the library facilitates targeted extraction of MS/MS-fragment intensities and assignment to the respective peptides.

The Venn diagrams are showing the significantly regulated proteins in the SWATH approach 1 hour and 6 hours after irradiation with 3 Gy vs. mock-irradiation for all three groups (controls, breast cancer patients harbouring the c.7271T>G substitution, and A-T patients).

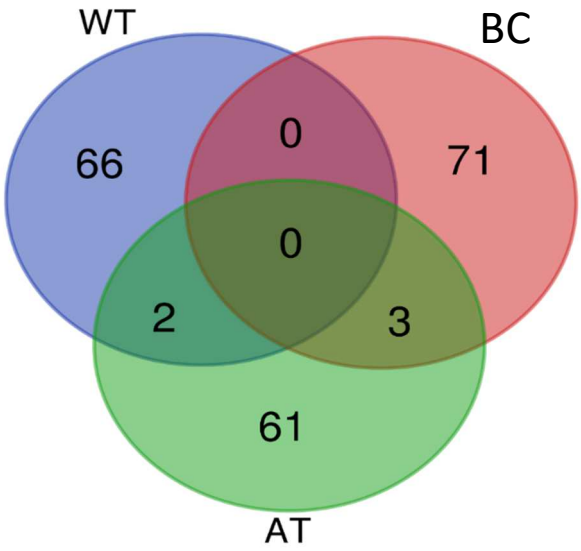


**Figure 11: SWATH Venn diagram of all significantly regulated proteins 1 hr after irradiation with 3 Gy versus mock-irradiation**

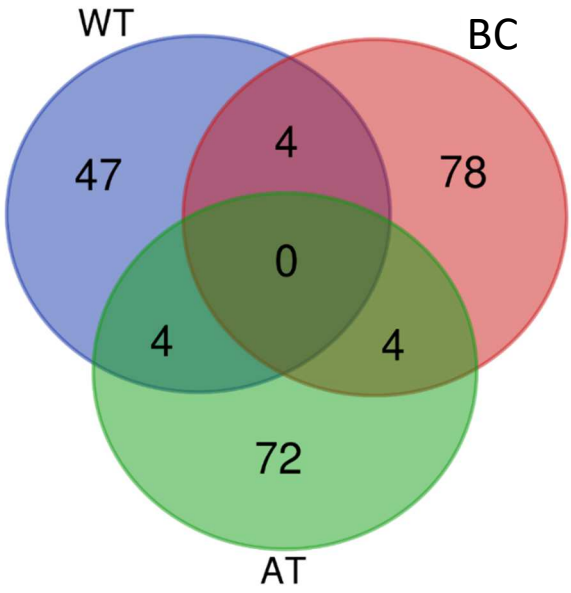


**Figure 12: SWATH Venn diagram of all significantly regulated proteins 6 hr after irradiation with 3 Gy**

The number of proteins that overlap between the different groups are very small, which can be explained by the fact that the individual samples of the breast cancer patients show a high variance. Interestingly, one protein – that was already described in the regulation of DNA mismatch repair (MMR) - showed a significant regulation after irradiation with 3 Gy. MSH6 showed a significant upregulation in the control cell lines 1 hour after irradiation compared to the cell lines derived from breast cancer patients carrying the c.7271T>G missense substitution and the cell lines derived from A-T patients.

For all proteins that were found in the SWATH approach, a GO-Enrichment analysis using DAVID v6.8 was carried out (Huang et al. 2009a, 2009b). Therefore all detected proteins were ranked according to their *p*-values and analysed to reduce these large protein lists into functionally related groups and to help to unravel the biological content of this data set. Beside significantly enriched protein groups that are involved in the regulation of metabolic/homeostatic cellular processes, transcription regulation and the regulation of cyclin-dependent protein serine/threonine kinase activity also a protein group involved in cell cycle control and different kinds of DNA repair pathways showed a significant enrichment at both 1 hr and 6 hrs after treatment; regulated proteins from this group are given in Table 12.

| Accession | Gene | Protein | Regulation upon irradiation[1] | | | Involved in process |
|---|---|---|---|---|---|---|
| | | | WT | BC | AT | |
| Q92878 | RAD50 | DNA repair protein RAD50 | ns | - | - | DSB |
| O60870 | KIN | DNA/RNA-binding protein KIN17 | ns | ns | - | DSB |
| P13010 | XRCC5 | X-ray repair cross-complementing protein 5 | + | ns | ns | DSB |
| P17844 | DDX5 | Probable ATP-dependent RNA helicase DDX5 | - | ns | ns | DSB |
| Q29RF7 | PDS5A | Sister chromatid cohesion protein PDS5 homolog A | + | ns | ns | DSB |
| P49959 | MRE11 | Double-strand break repair protein MRE11 | + | ns | ns | DSB |
| P09874 | PARP1 | Poly [ADP-ribose] polymerase 1 | ns | ns | - | BER |
| Q9NWY4 | CD027 | Histone PARylation factor 1 | ns | ns | - | BER |
| Q99459 | CDC5L | Cell division cycle 5-like protein | + | ns | ns | NER |
| Q01831 | XPC | DNA repair protein complementing XP-C cells | ns | ns | - | NER |
| P15927 | RFA2 | Replication protein A 32 kDa subunit | ns | ns | - | DSB, NER, BER |
| P18858 | DNLI1 | DNA-Ligase 1 | ns | ns | - | all kinds of DNA repair |
| Q9Y295 | DRG1 | Developmentally-regulated GTP-binding protein 1 | - | - | ns | Cell cycle arrest |
| [1]Regulations observed after 1 h are underlaid in grey. | | | | | | |
| +: significantly up-regulated | | | | | | |
| -: significantly down-regulated | | | | | | |

**Table 12: DNA repair proteins**

## 5.8. Targeted analysis using Western blotting 6 hours after irradiation vs. non-irradiation

Western Blot analyses were carried out for ATM, phosphorylated ATM (pATM) and one of the downstream targets of ATM – p53 and phosphorylated p53.

Western Blots showed no significant regulation after irradiation compared to the non-irradiated cell lines and compared between all different cell lines. However, a tendency is seen for p53, pATM and ATM. p53 is upregulated in the control cell lines compared to the A-T and breast cancer cell lines and pATM is slightly upregulated in the controls and breast cancer patients compared to the A-T patients. Interestingly, ATM is downregulated in the control cell lines compared to the A-T and breast cancer cell lines (Figure 13).

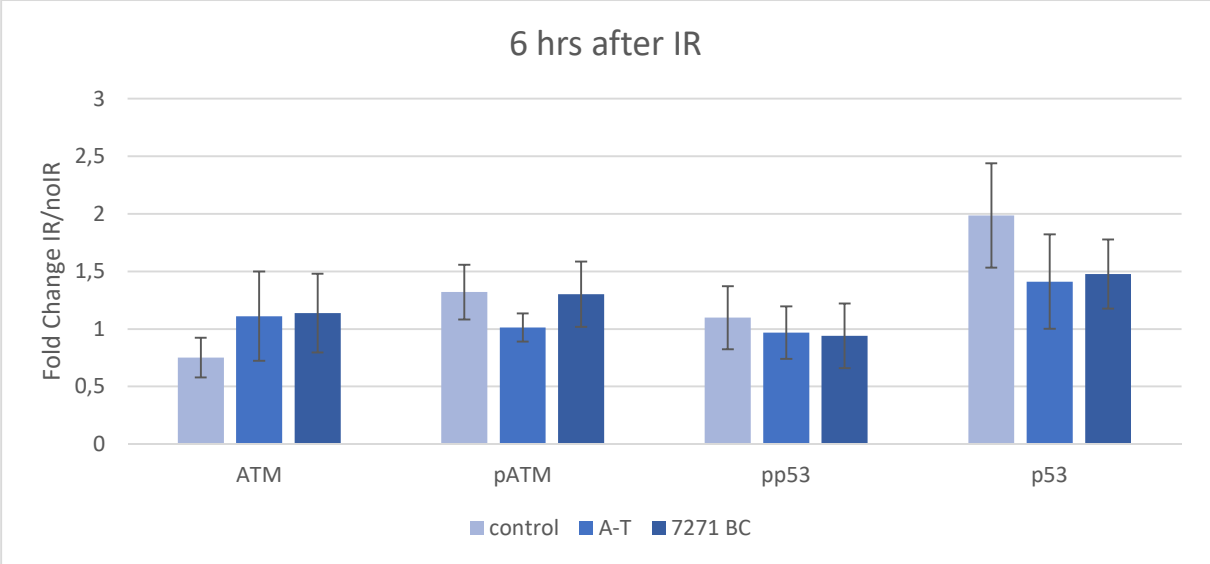


**Figure 13: Western Blot analysis for ATM, pATM, pp53 and p53 six hours after irradiation or mock-irradiation (*p≤0.05; four cell lines per group)**

A literature search lead to the hypothesis that there might be an export of a small fraction of ATM from the nucleus to the cytosol in a NEMO-dependent manner (Miyamoto 2011). Therefore, the cytosolic fraction was analysed by Western Blot analysis for ATM. However, there was no ATM protein detectable in the cytosolic fraction (Figure 14).

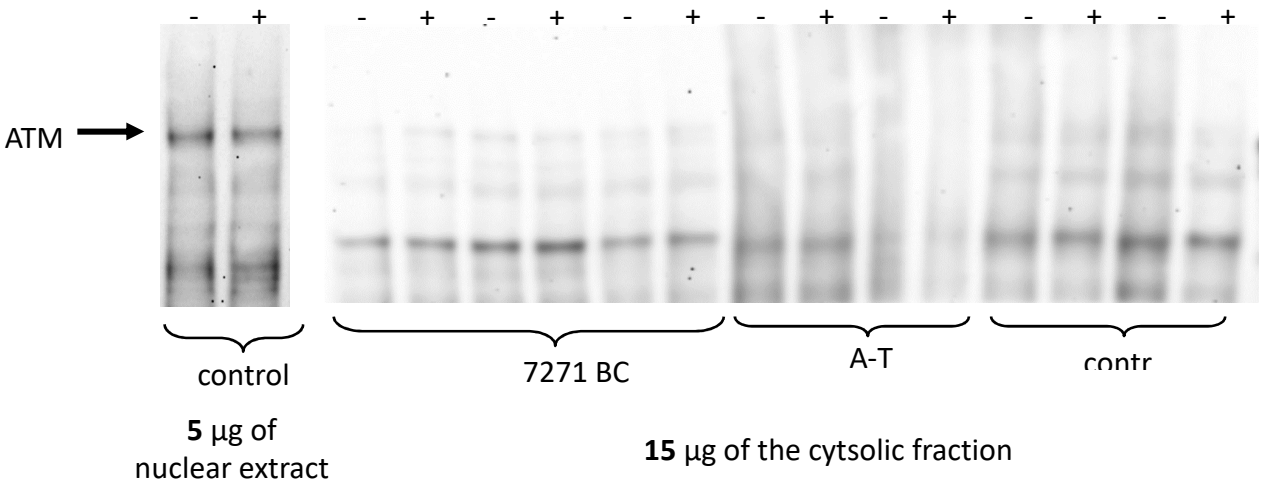


**Figure 14: Western Blot analysis for ATM in the nuclear and cytosolic fraction of one cell line from each group**

Additionally, based on the publication of Miyamoto in 2011, Western blot analysis with the nuclear and cytosolic fraction were carried out for NEMO and phosphorylated NEMO 6 hours after irradiation or non-irradiation. However, no significant regulation was detectable.

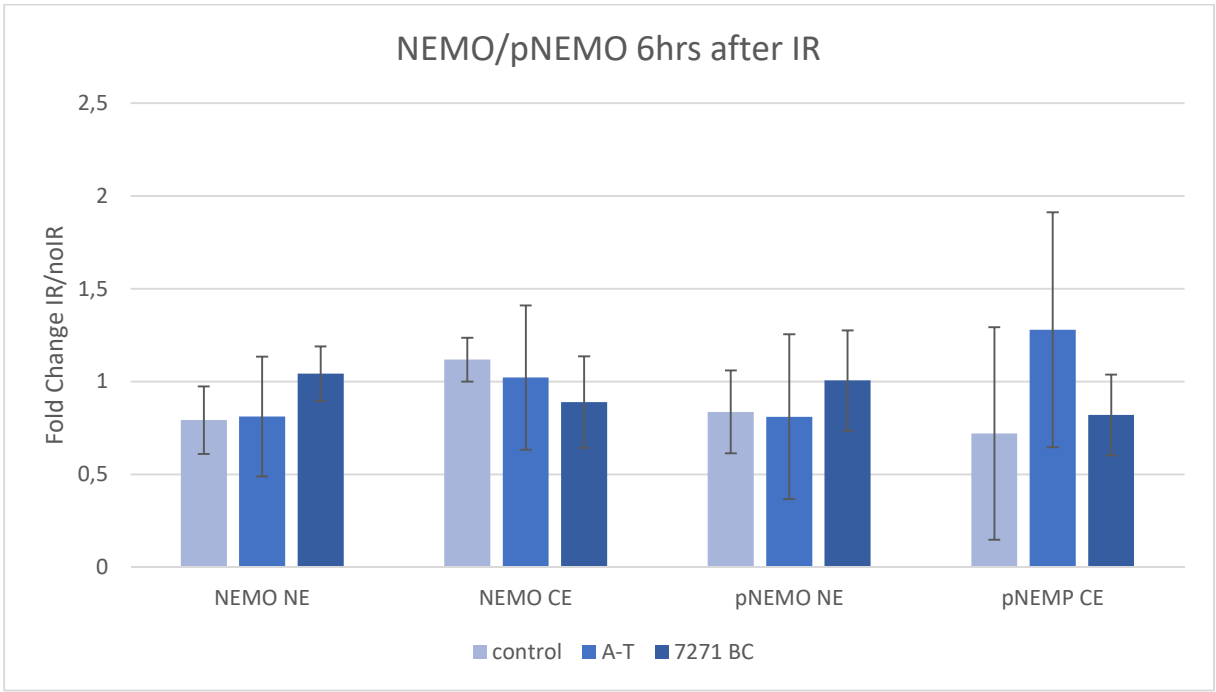


**Figure 15: Western Blot analysis for NEMO and pNMEO in the nuclear fraction**

## 5.9. Western Blot analysis for ATM, phosphorylated ATM and downstream targets at different time points

For further investigation the activation of ATM and its downstream targets in DNA damage response after irradiation Western Blot analysis was carried out with one control cell line and cells were harvested at different time points (0.5 hrs/1 hr/ 1.5 hrs) after irradiation. Figures 15 to 17 show the results of this timeline experiment in comparison to the 6-hour time point. Because only one control cell line was used for this experiment a standard deviation could not be calculated.

For ATM there is a slight downregulation from 0.5 hrs to 6 hrs detectable and the phosphorylated ATM shows clearly the highest fold change directly after irradiation at the 0.5-hrs time point (Figure 16).

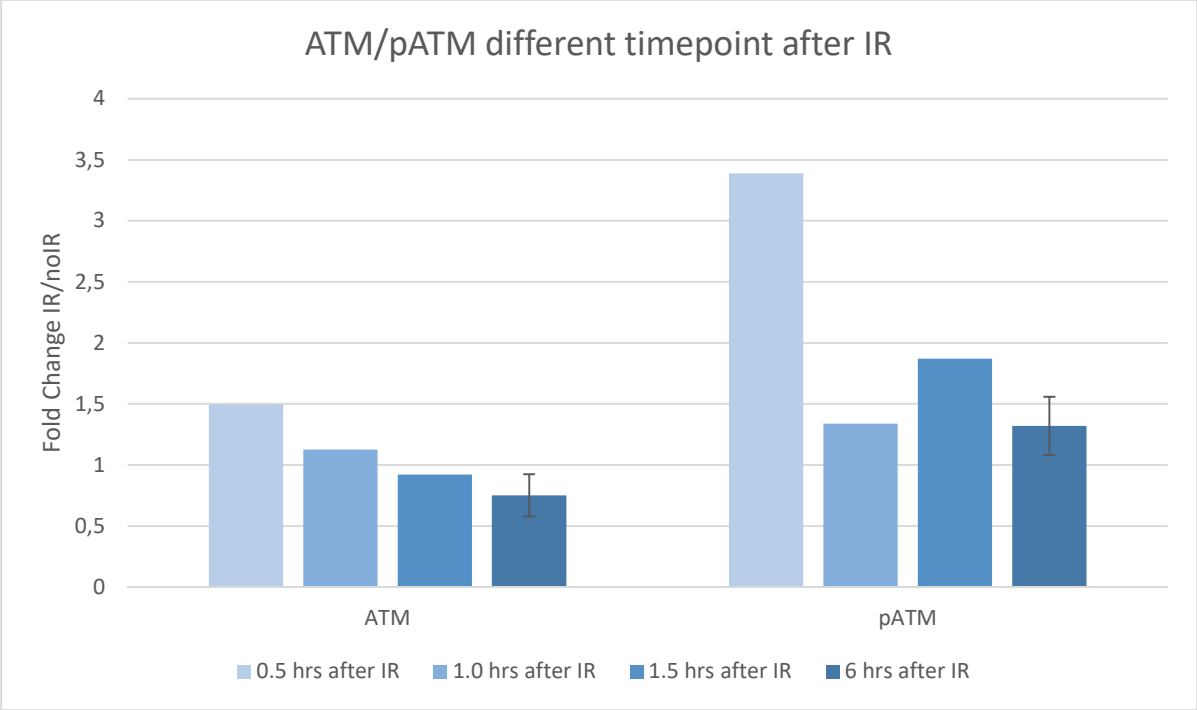


**Figure 16: Western Blot analysis for ATM and pATM in the nuclear fraction**

The downstream targets of ATM – the phosphorylated p53 and SMC1A – are illustrated in Figure 17. Phosphorylated p53 is upregulated 6-fold direct after irradiation (0.5-hrs time point) and shows the highest regulation at the 1-hr time point (14-fold change). The phosphorylated SMC1A shows the highest upregulation at the first time point (0.5-hrs with a six-fold change), which decreases slightly over time.

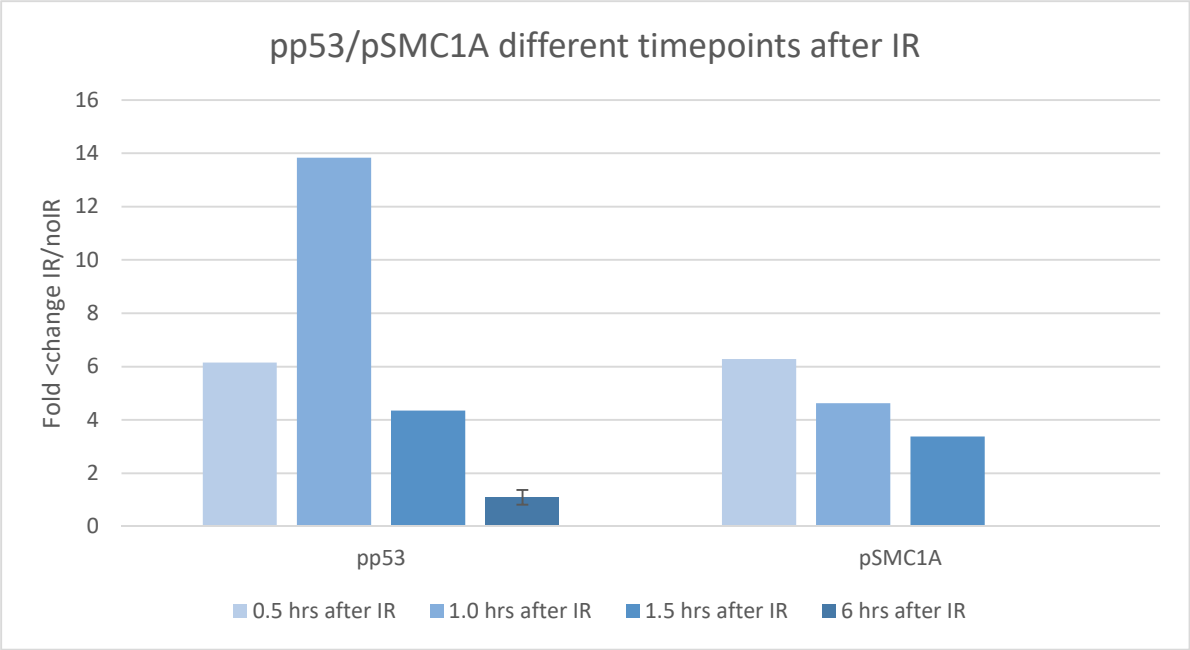


**Figure 17: Western Blot analysis for pp53 and pSMC1A in the nuclear fraction**

An additional Western Blot analysis for NEMO and phosphorylated NEMO shows an upregulation of NEMO and pNEMO in the nuclear fraction at the 1-hr time point, followed by a slow downregulation over time. Interestingly the Western Blot analysis for pNEMO in the cytosolic fraction shows a very high upregulation at the 1.5-hr time point compared to the earlier time points and the 6-hr time point (Figure 18).

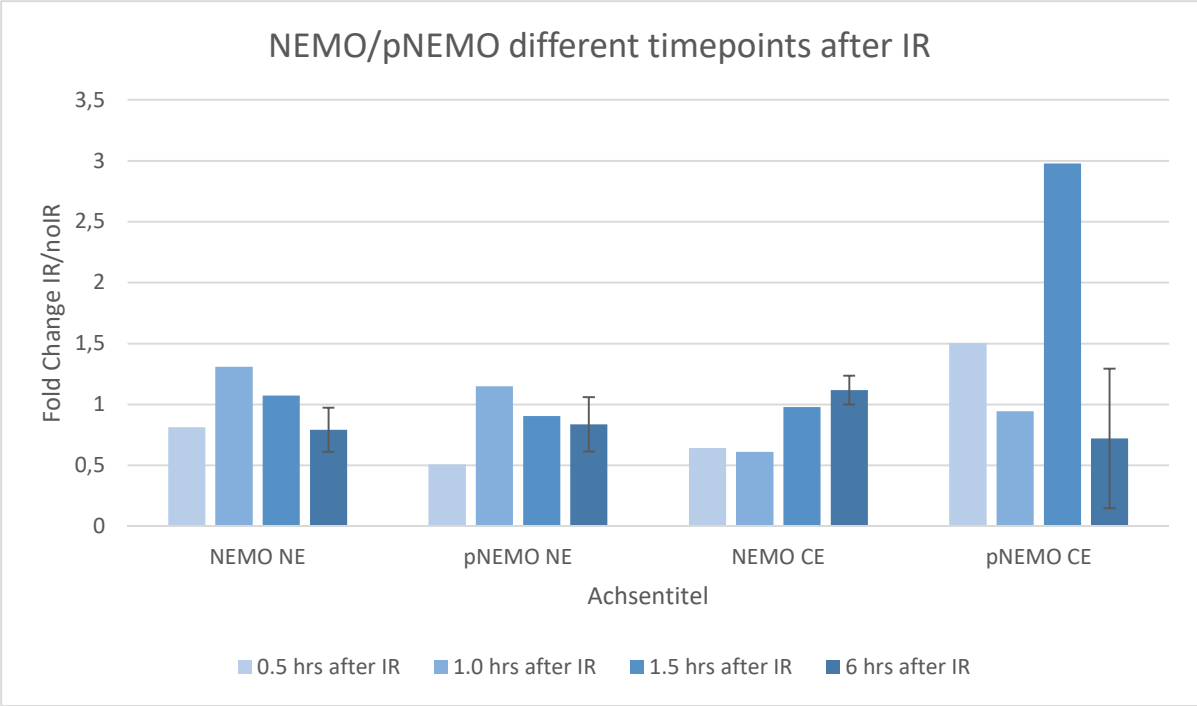


**Figure 18: Western Blot analysis for NEMO and pNEMO in the nuclear and cytosolic fraction at different time points**

## 5.10. Western Blot analysis 1 hr after irradiation for ATM, phosphorylated ATM and its downstream targets

Based on the time point experiment all cell lines were cultured again and harvested 1 hour after irradiation/non-irradiation. Western Blot analysis was carried out for ATM, phosphorylated ATM and the downstream targets in the DNA damage response machinery (pp53, pSMC1A and pNBS1). Figure 19 shows all Western Blot analyses at the 1-hour time point.

After DNA damage, ATM dimer separates into monomers. These monomers will be phosphorylated and the activated ATM is able to phosphorylate and activate downstream targets. pATM is not detectable in all cell lines derived from A-T patients and is upregulated in all other cell lines after irradiation with 3 Gy.

One of the downstream targets of ATM is p53. pp53 is highly upregulated in the control cell lines as well as in the cell lines derived from breast cancer patients with the c.7271T>G variant (15-20 fold). In contrast, the cell lines derived from A-T patients with common A-T mutations and from the patient harbouring the c.7271T>G variant in a homozygous state show only a slight upregulation (1-2 fold). The cell line with the c.7271T>G variant in a homozygous state was kindly provided by M. Taylor (University of Birmingham) and is a member of the family 109 (109-II-6; Stankovic et al. 1998). That cell line was added to the experimental setup to compare an additional c.7271T>G genotype.

Another downstream target of ATM is NBS1, which forms a multimeric complex with MRE11 and RAD50 after phosphorylation. After irradiation, pNBS1 is significantly upregulated in the control cell lines compared to the cell lines derived from the A-T patients. In all other cell lines phosphorylated NBS1 is also upregulated after irradiation but there is no significant difference.

A second downstream target of ATM is SMC1. It was shown to be a target of the ATM kinase with phosphorylation of Ser957 and Ser966 after ionizing radiation (Kitagawa et al. 2004). In the present study all cell lines show a significant upregulation after irradiation. The control cell lines are significantly upregulated compared to the A-T and c.7271 A-T cell lines. In addition, the cell lines derived from breast cancer patients harbouring the heterozygous c.7271T>G variation are significantly upregulated compared to the c.7271T>G homozygous cell lines.

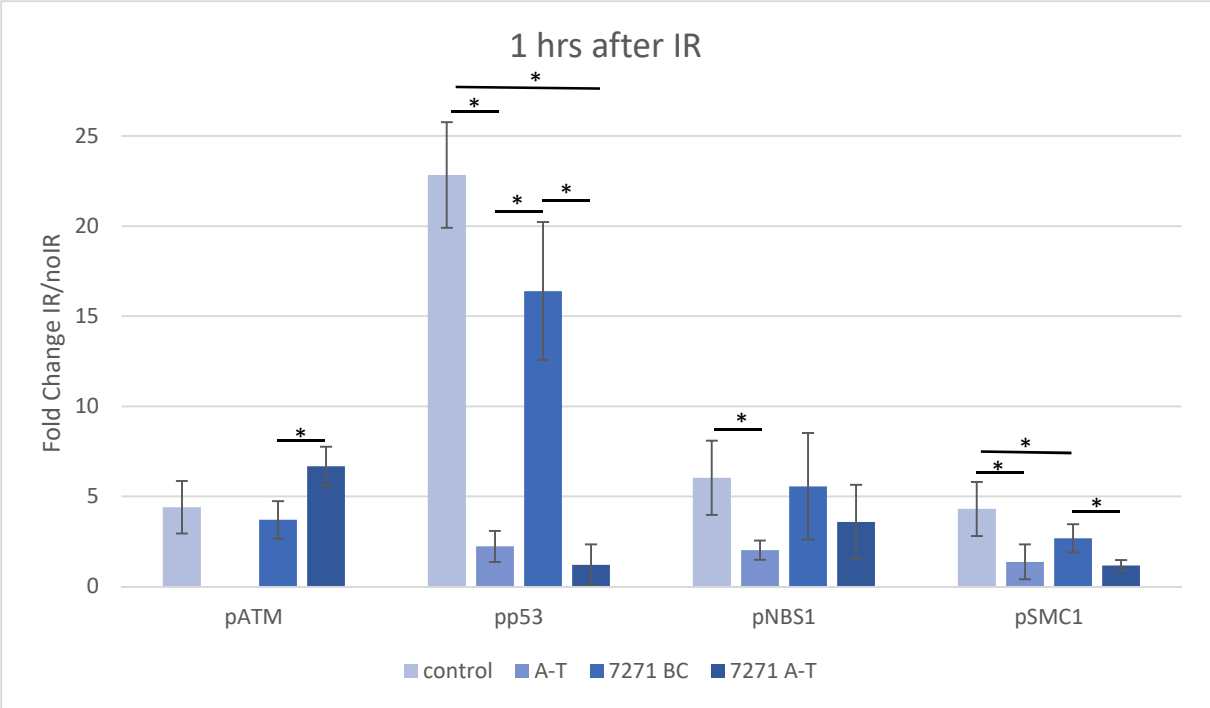


**Figure 19: Western Blot analysis for pATM, pp53, pNBS1 and pSMC1 in the nuclear fraction at the one hour time point (*p≤0.05 (one-way ANOVA with subsequent Tukey´s post hoc T-test))**

# 6. Discussion

## 6.1 Cell growth, cell viability, cell death, cell cycle checkpoint and chromosomal breaks after irradiation with 3 Gy

In proliferating cells, the cell cycle is an ordered series of events that cells pass through. Each cell cycle consists of two different stages: the Interphase, which comprises the G1, S and G2 phase, respectively, and the Mitosis-phase (M-phase), in which a cell is divided into two daughter cells. At the transition between G1/S-phase, G2/M-phase and at the end of the S-phase, there are special checkpoints controlled by cyclin-dependent kinase complexes. These complexes monitor the integrity of the specific cell cycle event before allowing cells to progress into the next phase. Different endogenous or exogenous agents can damage DNA in the cell and, therefore, these cell cycle checkpoints function as a control point to arrest the dividing cell and to determine whether the damage can be repaired and the cell can progress thru the cell cycle or cannot be repaired and the cell has to undergo apoptosis. Defects in cell cycle checkpoint recognition and/or disturbed DNA damage repair machinery can lead to an accumulation of DNA breaks and/or mutations in the DNA, which can lead to uncontrolled cell division and an increased incidence of cancer. The increased cellular radiosensitivity, cell cycle checkpoint defects and chromosomal instability in AT patients results in an increased risk of malignancy. Since 1991, it has been suggested that blood relatives of A-T patients show an increased risk of cancer, especially breast cancer. Taking into account all the published data, it seems that the *ATM* gene is associated with a moderate risk, but it is still not clear if *ATM* mutations can act multiplicatively and impact the response to radiotherapy.

Therefore, ionizing radiation of lymphoblastoid cell lines derived from A-T patients, carrying compound heterozygous mutations in the *ATM* gene, or breast cancer patients harbouring the heterozygous c.7271T>G substitution in the *ATM* gene, might illustrate the impact of such mutations on cell growth, cell viability and chromosomal breaks. All cell lines were irradiated with 3 Gy or mock-irradiated and analysed to investigate cell growth by cell counting, differentiating between late apoptotic/necrotic or early apoptotic cell using Annexin-PI staining, monitoring of the percentage of cells in each cell cycle phase using PI-staining and, finally, counting chromosomal breaks by karyotype analysis.

Cell counting after irradiation and mock-irradiation shows for all irradiated cell lines a decreasing cell count, which can be due to cell cycle arrest or an increase in apoptotic or necrotic cells. For further investigation, Annexin-PI staining was carried out followed by flow cytometry. This method could confirm, that the fraction of cells that undergo necrosis and apoptosis after irradiation increased in all cells lines tested. The control cell lines show a slight increase in necrotic and apoptotic cells, the cell lines from AT patients show a significant increase in necrotic cells and a slight decrease in apoptotic cells, while the cell lines derived from breast cancer patients show an intermediate increase in apoptotic and necrotic cells. Comparing all three different groups after irradiation shows that cell lines from AT patients show the highest percentage of necrotic cells compared to the controls, while cells from

breast cancer patients show only a modest increase in apoptotic cells in comparison to the control cell lines. The percentage of apoptotic cells was the highest in the control group, followed by the cell lines from AT patients and breast cancer patients, which differed only slightly. This experiment demonstrated that cells from AT patients, whose IR-induced DNA damage could not be repaired by the DNA repair machinery due to their defective ATM protein, undergo necrosis instead of apoptosis. Compared to that, the control cell lines show much less dead cells and most of them undergo the controlled cell death (apoptosis). Cells from breast cancer patients show a slightly higher percentage of apoptotic and necrotic cells compared to the controls, but do not behave anywhere like the cells from AT patients.

DNA damage leads to an arrest of the cells at one of the cell cycle checkpoints. A PI staining was carried out to further investigate the effect of different ATM mutations on the cell cycle arrest. After irradiation all cell lines were stained and the percentage of cells in each cell cycle phase was measured. The irradiation with 3 Gy shows in the G1 phase no alterations in the control cell lines and in the breast cancer cell lines compared to the mock-irradiated cells. Cell lines from AT patients show a lower percentage of cells in the G1 phase after irradiation, which is significantly lower compared to the control ($p = 0.13*10-2$) and the breast cancer cells ($p = 0.43*10-4$). In addition, there is no difference between the controls and the cell lines derived from breast cancer patients after irradiation with 3 Gy. In S phase, all cell lines show a significant decrease after ionizing radiation, but there is no difference between the groups with or without irradiation. In contrast, the G2/M phase shows a significant increase in cells after irradiation in the controls, the AT patients as well as the breast cancer patients. Additionally, there is a significant difference between the A-T cell lines after irradiation compared to the controls ($p = 0.4*10-3$) and the c.7271T>G cell lines ($p = 0.58*10-3$). Irradiation with ionizing radiation on control cell lines leads to DNA damage resulting in an arrest at any of the three cell cycle checkpoints and after DNA damage recognition and repair normal cells proceed in the cell cycle. This experiment shows that all three groups behave the same at the S phase and G2/M phase checkpoint, but that there are differences between the control and breast cancer group compared to the AT group. Cells harbouring compound heterozygous mutations in the ATM gene that lead to an A-T phenotype show a defect in the G1 checkpoint (significant lower percentage of cells compared to controls and heterozygous c.7271T>G cells) and a significant accumulation of cells in the G2/M phase compared with the control and breast cancer cell lines. A defective G1 checkpoint due to an absent activation of p53 was first published in 1992 by Kastan et al. (Kastan et al. 1992) and could be confirmed with this experiment.

One of the common features in A-T is an accumulation of chromosomal breaks after ionizing radiation. Therefore, the third experiment involved Giemsa staining of the chromosomes in metaphase to count the number of chromosomal breaks after ionizing radiation. This had been already carried out and published by Waddell et al. in 2006 (Waddell et al. 2006). As in that paper, the number of chromosomal breaks per metaphase was higher in the A-T and c.7271T>G cells compared to the control cell line. Taking into account the small number of

analysed metaphases, the cell lines from breast cancer patients harbouring a c.7271T>G substitution show a higher percentage of induced chromosomal aberrations compared to the controls but do not behave like the cells derived from A-T patients with compound heterozygous ATM mutations.

## 6.2. DIGE Analysis with nuclei enriched cell fractions

DIGE analysis was carried out to further investigate differences between cell lines derived from A-T patients and breast cancer patients harbouring a c.7271T>G substitution, respectively, on the proteome level. After induction of DNA damage by ionizing radiation, normal cells recognize this damage, arrest at one of the cell cycle checkpoints and recruit the repair machinery at the DNA damage site. Due to their different mutation status in the *ATM* gene a different reaction in the DNA damage response machinery is suspected for the different kinds of cell lines. To proof this hypothesis, DIGE analysis was carried out for all cell lines, which allows a quantitative and qualitative examination of the proteome. However, whole cell lysate represents a too complex mixture to analyse. Since the main response machinery for ionizing radiation induced DNA repair is located in the nucleus, a protocol was carried out for cell lysis and nuclei enrichment. An extensive literature search provided three different protocols, which were tested and followed by Western Blot analysis to determine the purity of the subcellular fractions. All three protocols showed an enrichment of the nuclear fraction with a different quantity and quality in enrichment and purity. The best results were obtained with the protocol published by Rascle (Rascle et al. 2003). The Western Blot analysis shows a sufficient enrichment of nuclei in the subcellular fraction, which is rarely contaminated by cytosol.

For the DIGE analysis all samples were labelled with fluorescent dyes (non-irradiated with Cy5, irradiated with Cy3 and a combination of non-irradiated and irradiated with Cy2). After the computer-assisted comparison (irradiated vs non-irradiated in each group) all significantly regulated spots were evaluated, the gels were silver stained and all regulated spots were picked. These spots were washed, destained and analysed by mass spectrometry. Compared with the controls and the breast cancer cell lines the AT patients showed more regulated spots after irradiation with 3 Gy (Figure 10). Approximately half of the regulated spots could be analysed with mass spectrometry and 64 proteins could be identified in the control cell lines, 42 for the cell lines derived from A-T patients and 43 proteins could be identified with this approach for the cell lines harbouring the heterozygous c.7271T>G variant. Although there was a nuclei enrichment carried out prior to DIGE analysis only a part of the identified proteins are of nuclear origin.

Prefractionation can reduce the complexity of a sample and increase the visibility of minor proteins. Therefore, the nuclei enrichment protocol was established and used prior to DIGE analysis. However, the mass spectrometry results show that all samples were contaminated with proteins from the endoplasmatic reticulum and mitochondria. This can be improved with an adapted nuclei purification protocol including different sucrose gradients which increase

the purity of the nuclei. However, a better purification of the nuclei can result in a destabilisation of the nuclear membrane and, therefore, a loss of nuclear material and proteins. In addition, the DIGE approach can be improved to increase the resolution and, therefore, avoid the problem that there is more than one protein per spot. The resolution of the first dimension can be increased by using strips with smaller pH gradients (pH 3-6/ pH 5-8/ pH 7-10) instead of pH gradient from 3-10. For the second dimension, gradient gels or gels with a lower or higher percentage of acrylamide can improve the resolution due to a different pore size of the gel.

Most of the proteins that showed a significant regulation in all three groups comparing non-irradiated vs. irradiated cells were proteins involved mRNA processing, RNA splicing as well as transcription factors and proteins that are part of the cytoskeleton and nuclear lamina.

A gel spot that was significantly downregulated in both, the control and AT cell lines, contained the protein MRE11. MRE11 is one of three members of the MRN complex that is recruited to the site of DNA damage by binding active histone H2AX (yH2AX) (Jager et al. 2001; Paull und Lee 2005). The active MRN complex enables the recruiting of ATM at the DNA double-strand break as well as the activation of ATM by monomerization and autophosphorylation (Bakkenist und Kastan 2003). A downregulation of MRE11 after ionizing radiation can be due to a phosphorylation of MRE11. When proteins are phosphorylated, the protein pI will shift to a more acidic region, which leads to a shifting of the protein spot in the 2D gel and, therefore, a downregulation of the non-phosphorylated protein spot.

Another protein that is involved in DNA damage repair is SMC1A. SMC1A is a member of the cohesin complex – a chromosome-associated multisubunit protein complex that is mainly involved in sister chromatid cohesion and, therefore, is considered essential for chromosome segregation in dividing cells. Furthermore, studies of cohesin mutants in yeast suggest a role for this complex in genome integrity and DNA repair, which was further supported by Kim et al., who could demonstrate an ATM-dependent phosphorylation of SMC1A after ionizing radiation (Kim et al. 2002). SMC1A was also downregulated in the control cell lines after ionizing radiation with 3 Gy. This downregulation can also be due to the shifting of the phosphorylated form of SMC1A in the 2D gel.

The cell lines derived from the AT patients also showed an upregulation of RAD23B – a protein that is involved in Nucleotide Excision Repair (NER). RAD23B builds a complex together with XPC and this protein complex recognizes DNA lesions and is required for the efficient recruitment of all the following NER proteins (Fousteri und Mullenders 2008). It is already published and could also be shown in this work that AT patients accumulate a lot more chromosomal breaks and DNA lesions compared to controls and breast cancer patients, which results in a higher risk of cancer. Nevertheless, these cells are able to survive and to repair DNA damages which could be due to other pathways – excluding ATM – or due to other kind of DNA repair – for example nucleotide excision repair (NER) or homologous recombination (HR).

Interestingly, the control cell lines as well as the cell lines derived from breast cancer patients showed an opposed regulation of NONO. This protein was significantly downregulated in the control cell lines and upregulated in the cell lines harbouring a 7271T>G *ATM* substitution. NONO forms heterodimers with SFPQ, which are localized in nuclear bodies called paraspeckles and these protein complexes are involved in DNA and RNA metabolism (Shav-Tal und Zipori 2002). In addition, Salton et al. (2010) suggested that NONO and SFPQ are early response proteins after DNA damage and are directly involved in DSB repair via the NHEJ pathway (Salton et al. 2010).

## 6.3. Western Blot Analysis 6 hours and 1 hour after irradiation with 3 Gy

One of the most sensitive and specific tests for diagnosing A-T is immunoblotting of the ATM protein (Chun et al. 2003). About 90% of the patients do not show detectable ATM protein in this test, around 10% have trace amounts of protein and ~1% show normal ATM protein levels but no kinase activity (so called “kinase-dead”). To measure the activity of the ATM protein usually immunoblotting for ATM-dependent phosphorylation target proteins such as p53 (Ser15), SMC1 (Ser966) or ATM itself (Ser1981) is employed.

First, Western Blot analysis was carried out for ATM, phosphorylated ATM (pATM) and one of the downstream targets of ATM – p53 and phosphorylated p53 at 6 hours after irradiation parallel to the DIGE approach. After irradiation with 3 Gy the immunoblotting of ATM showed no significant differences between the control cell lines as well as the cell lines derived from A-T patients and breast cancer patients harbouring the heterozygous c.7271T>G substitution. But interestingly, ATM is downregulated in the control cell lines compared to the A-T and breast cancer cell lines. A literature search leads to the hypothesis that there is maybe an export of a small fraction of ATM from the nucleus to the cytosol in a NEMO-dependent manner (Miyamoto 2011). Therefore, the cytosolic fraction was analysed by Western Blot analysis for ATM, but there was no ATM protein detectable. This could be due to the small amount of ATM protein in a whole cell lysate and could be optimized with an immunoprecipitation approach against ATM. Additionally, based on the publication of Miyamoto in 2011 Western Blot analysis with the nuclear and cytosolic fraction were carried out for NEMO and phosphorylated NEMO 6 hours after irradiation or non-irradiation, but no significant regulation of NEMO or pNEMO could be detected.

To further investigate the activation of ATM and its downstream targets in DNA damage response after irradiation, a timeline experiment was carried out. A second Western Blot was set up with one control cell line which was harvested at different time points (0.5 hrs/1 hrs/ 1.5 hrs) after irradiation with 3 Gy. The activation of ATM and its downstream targets was much more detectable in this timeline experiment compared to the 6 hour time point. The phosphorylated ATM shows clearly the highest fold change directly after irradiation; at the

0.5-hr time point, the phosphorylated p53 is upregulated 6-fold and shows the highest regulation at the 1-hr time point (14-fold change), while the phosphorylated SMC1A shows the highest upregulation at the first time point (0.5 hrs with a 6-fold change), which decreases slightly over time. Furthermore, an additional Western Blot analysis for NEMO and phosphorylated NEMO shows an upregulation of NEMO and pNEMO in the nuclear fraction at the 1-hr time point, followed by a slow downregulation over time. Interestingly the Western Blot analysis for pNEMO in the cytosolic fraction shows a very high upregulation at the 1.5-hr time point compared to the earlier time points and the 6-hr time point. This experiment demonstrates that at the 6-hr time point most of the ATM kinase activity is already downregulated. Accordingly, the timeline experiment shows that the time point for the DIGE approach as well as the Western Blot analysis might be too late and therefore the Western Blot analyses were set up again.

All cell lines were cultivated, irradiated with 3 Gy, harvested one hour after irradiation and all downstream targets were analysed again by Western Blot analysis. At the 1-hour time point, pATM is not detectable in the cell lines derived from A-T patients and is upregulated in all other cell lines after irradiation with 3 Gy with no significant difference between control and heterozygous c.7271T>G cell lines. One of the downstream targets of ATM is p53. It is highly upregulated in the control cell lines as well as in the cell lines derived from breast cancer patients heterozygous for the c.7271T>G variant (15-20 fold). Interestingly, both the A-T and the cell line homozygous for the c.7271T>G variant show only a slight upregulation (1-2 fold) However, Western blots for phosphorylated p53 show a significant difference between the control cell lines and the c.7271T>G breast cancer patients compared to the cell lines derived from A-T patients harbouring common A-T mutations or the homozygous c.7271T>G variant. Another downstream target of ATM is NBS1 that is significantly downregulated in the A-T cell lines. A third downstream target of ATM is SMC1A and in this experiment all cell lines show a significant upregulation after irradiation. SMCA1 is significantly upregulated in the control cell lines compared to the A-T and homozygous c.7271T>G cell lines. In addition, in the cell lines derived from breast cancer patients harbouring the heterozygous c.7271T>G variation SMCA1 is significantly upregulated compared to the c.7271T>G homozygous cell lines.

A comparison of these results to the literature is not easy due to an ongoing discussion about the behaviour of phosphorylated ATM and their downstream targets after irradiation in the heterozygous c.7271T>G cell lines derived from breast cancer patients. In 1998, Stankovic published a family (family 109) with three AT patients showing mild clinical symptoms and the homozygous mutation c.7271T>G in the *ATM* gene (Stankovic et al. 1998). The whole family had a history of familial breast cancer including the mother of the three AT patients, who was heterozygous for the c.7271T>G substitution. Stankovic postulated that the detected mutant ATM protein shows residual function and, therefore, leads to a ‘dose response’ effect in which the degree of mildness depends on the level of mutant but functional ATM protein. In 2001 Stewart further investigated family 109 and could demonstrate a full length ATM protein for all cell lines derived from heterozygous and homozygous carriers of the c.7271T>G

substitution, a weak autophosphorylation and residual kinase activity (phosphorylation for p53, NBS1 and MRE11) of about 4-6% in the homozygous cell lines after irradiation with 5 Gy (Stewart et al. 2001). In 2002, Chenevix-Trench published a second family carrying the c.7271T>G ATM variant (family A) by genotyping the kConFab families – families at high risk for breast cancer (Chenevix-Trench et al. 2002). They analysed cell lines derived of family 109 – with homozygous and heterozygous c.7271T>G carriers – and cell lines of family A – with only heterozygous c.7271T<G carriers. After irradiation with 6 Gy, Western Blot analysis revealed full length ATM protein for homozygous carriers of c.7271T>G, the control cell lines and c.7271T>G heterozygous carriers. However, additional Western Blot analysis for downstream targets of ATM showed a completely abolished p53 phosphorylation in c.7271T>G homozygous carriers and the c.7271T>G heterozygous carriers had only 15-25 % of normal kinase activity – measured by p53 and BRCA1 phosphorylation - compared to normal controls. Based on these results, which were in contrast to the previously published results of Stankovic (1998) and Stewart (2001), Chenevix-Trench hypothesized that the c.7271T>G mutation acts in dominant-negative manner and, therefore, the wild-type enzyme is unable to function normally in the presence of the altered protein, due to for example competition effects for binding partners, substrates and regulators and therefore increases the risk of breast cancer in this women. In 2006, Waddell further investigated the heterozygous c.7271T>G carriers using microarray and Western blot analysis. Western Blot analyses of p53 and phosphorylated p53 (Ser15) were carried out to study radiosensitivity after irradiation of the cell lines with 5 Gy. The heterozygous and homozygous c.7271T>G carriers showed a wide range of response and interestingly Waddell could not confirm the results that Chenevix-Trench had published in 2002. In contrast to the previously reported results the phosphorylation of p53 at Ser15 was comparable between the wild-type cell lines and the c.7271T>G heterozygotes. The authors justified this discrepancy with the assumption that in the previous study they had used freshly established lymphoblastoid cell lines and that the previously postulated dominant negative effect could be influenced by a high passage number. Furthermore, they discussed an ATM-independent stabilization of p53 affected by cell culture density. Nevertheless, the heterozygous c.7271T>G carriers showed higher levels of p53 and phosphorylated p53, which might be due to the activation of other cellular DNA damage repair pathways after ionizing radiation. The use of other DNA damage pathways is supported by the observation that c.7271T>G homozygotes show the highest incidence of chromosomal aberrations, followed by heterozygous carriers and, thereafter, wild-type cells.

The Western blot analysis carried out here could not confirm the dominant negative effect in the cell lines harbouring the heterozygous c.7271T>G substitution postulated by Chenevix-Trench and Waddell. All experiments show that cell lines harbouring the c.7271T>G substitution in a heterozygous state act between the control cell lines and the cell lines derived from AT patients harbouring truncating mutations or the c.7271T>G variant in a homozygous state. Nevertheless, the pedigree of the family A published 2002 by Chenevix-Trench shows that the breast cancer is inherited with the same haplotype. One explanation could be that a

second mutation in another gene (located in this haplotype) acts as a modifier or an additional genetic factor (digenic inheritance). The haplotype could be further investigated for example by next generation sequencing – a new method to sequence whole exome or genomes as well as specific parts of the genome in a fast and cost effective manner. Additionally, the two-hit hypothesis – first published by Knudson 1971 could be also a possible explanation (Knudson, JR 1971). Knudson used a statistical model for retinoblastoma and hypothesized that one mutant allele is inherited and the other one is generated somatically during growth and therefore the cancer susceptibility phenotype is inherited in a dominant manner. Taking into account this hypothesis an investigation of breast tumor material by Western blot and/or DNA sequencing could give new insights in this matter.

In addition the time line experiment showed that the strongest response after irradiation with 3 Gy was at the one-hour time point. It would be interesting to repeat the DIGE approach at this time point to investigate the differences between all four groups (controls, AT patients, c.7271T>G heterozygous and c.7271T>G homozygous).

## 6.4. SWATH Analysis

In comparison to the 2D-PAGE analyses, the SWATH-MS approach yields a much larger set of quantified proteins with virtually no missing values. Therefore, it is suited much better for quantitative analyses then typical data-dependent approaches (Zhu et al. 2014). However, modified peptides are filtered out prior to quantification – even if they had been identified in the (data dependent) library runs and, therefore, the quantification in the SWATH-MS analysis is based solely on non-modified peptides. Additionally, protein variants such as truncated proteins, protein isoforms, modified proteins, etc. are often not detectable using bottom-up approaches (Lottspeich 2009). Therefore, the SWATH-technology is a truly orthogonal analysis approach to the gel-based top-down analysis conducted by 2D-PAGE.

The combination of top-down 2D-gel-based (top-down) and shotgun-DIA-based analyses has clear advantages over the frequently used, mostly shotgun-based stable isotope labelling strategies. These methodologies - such as SILAC, iTRAQ, TMT - use the incorporation of stable isotope-coded moieties into proteins or peptides metabolically or by chemical means (Chahrour et al. 2015) and this allows the subsequent combination of two or more samples (so-called „multiplexing“) and therefore minimizes the problem of sample-specific losses due to low reproducibility of downstream separation and detection techniques. The quantification is based on mass spectrometry either on the MS (e.g. for SILAC, ICAT, ICPL) or the MS/MS-level (e.g. for iTRAQ, TMT). Multiplexing with MS-level-based quantification is accompanied by the reduction of sensitivity due to peak splitting on the MS-level. This does not happen if you are using MS/MS-based techniques which typically require higher scan rates of the used mass spectrometers. All these methods avoid the missing-data problem (Roderick J. A. Little, Donald B. Rubin 2002) as long as the maximum number of analysed samples does not exceed the possible level of multiplexing including biological and technical replicates. If more than ten samples (as in this study) are to be compared, the missing data problem arises again and

drastically complicates data interpretation. Additionally, multiplexing using stable isotope labelling strategies is cost intensive and thereby limiting the number of samples/replicates to be investigated.

SWATH analysis was carried out as an additional approach to analyse differences in the nuclear lysates one hour and six hours after irradiation with ionizing radiation. A DAVID analysis was carried out to cluster these proteins into functionally related groups and to help to unravel the biological content out of this data set. Beside protein groups that are involved in the regulation of metabolic/homeostatic cellular processes, transcription regulation and the regulation of cyclin-dependent protein serine/threonine kinase activity also protein that are involved in cell cycle control and different kinds of DNA repair pathways showed up. Interestingly the comparison of the proteins that are regulated six hours after irradiation within each of the three groups (controls, A-T patients, breast cancer patients harbouring the c.7271T>G substitution) shows that in the control cell lines proteins that are involved in DSB – like XRCC5, PDS5A, MRE11 and CDCL5 – are upregulated after irradiation and show no regulation upon irradiation in the cell lines derived from A-T patients or breast cancer patients. Interestingly RAD50 – one member of the MRN complex – is downregulated in the breast cancer and in the A-T patients after irradiation.

However, of particular interest is the reduced regulation of proteins involved in Nucleotide Extension Repair (NER) and DNA mismatch repair (MMR) in the c.7271T>G heterozygous cell lines compared to the controls. Already in 2009, Zhang published an overview connecting nucleotide extension repair (NER) and DNA mismatch repair to double-strand DNA breakage repair (Zhang et al. 2009). Figure 1 in the paper of Zhang et al. shows the proposed linkage between NER/MMR and double-strand DNA repair. Interestingly, a few proteins described in the present work have been found to be regulated in the same direction by both DIGE and SWATH. They include MSH2 and MSH6, which build a heterodimeric complex with misrepair-recognition specificity in MMR. One hour after irradiation, MSH6 is upregulated in the control cell lines, but significantly downregulated in the AT and in the c.7271T>G heterozygous cell lines. Interestingly, in 2011, Romeo et al. could show a link between ATM and the MMR pathway. They could demonstrate that the hMLH1 protein – that is part of the of the MMR pathway - is phosphorylated at Ser406 by BRCA1 in an ATM-dependent manner (Romeo et al. 2011). Afterwards hMLH1 is building a heterodimer with PMS2 (= MutL alpha). This heterodimer is recruited to mismatch pairs with damaged bases after these were recognized by the two other heterodimers MutS alpha (MSH2 and MSH6) and MutS beta (MSH2 and MSH3) and leads to the activation of the endonuclease activity of PMS2. Beside their involvement in MMR, Shahi et al. (2011) could also show an interaction of MSH6 with KU70 – one of the two key regulatory subunits of the DNA-dependent protein kinase, which plays an essential role in DNA double-strand break repair (Shahi et al. 2011). Shahi et al. also demonstrated a co-localization of MSH6 with activated and phosphorylated H2AX (γH2AX) – one of the downstream targets of ATM and also a key player in double strand break recognition. Therefore, a co-immunoprecipitation as well as Western Blot for phosphorylated

hMLH1 after irradiation with ionizing radiation would give new insights in this linkage between ATM and the MMR pathway.

Another method to further investigate the differences in NER between control cell lines and the cell lines of breast cancer patients harbouring the c.7271T>G substitution would be an assay established by Rubbi and Milner in 2001 (Rubbi und Milner 2001). During NER, transient stretches of single-stranded DNA are generated and Rubbi and Milner developed a method, which allows single cell microscopic analysis and kinetic analysis of the DNA repair response based on labelling of the double stranded DNA with BrdU and using an anti-BrdU antibody to detect the single-stranded DNA generated in NER.

Furthermore, interestingly another protein RAD23B – which is also connected to NER – was downregulated in the cell lines derived from breast cancer patients compared to the control cell lines as well as to the cell lines derived from AT patients. In 2009, Zhao et al. could show an interaction of MutS beta –the complex of MSH2 and MSH6 – with XPA-RPA or XPC-RAD23B in the process of DNA interstrand crosslinks (Zhao et al. 2009). Already in the DIGE analysis RAD23B was significantly upregulated in the cell lines derived from AT patients compared to the controls and the cell lines harbouring the c.7271T>G heterozygous mutation. At the 1-hour time point, SWATH analysis showed a significant upregulation of RAD23B in both controls and AT patients, which had disappeared at the 6-hr time point. This regulation of RAD23B gives an additional hint to a restricted function of NER and maybe MMR in the cell lines derived from the breast cancer patients harbouring the c.7271T>G substitution, which should be further investigated by Western Blot analysis of key players in this pathway and additional methods as described by Rubbi and Milner (Rubbi und Milner 2001).

# References


Ahmed, M.; Rahman, N. (2006): ATM and breast cancer susceptibility. In: *Oncogene* 25 (43), S. 5906–5911. DOI: 10.1038/sj.onc.1209873.

Alterman, Neora; Fattal-Valevski, Aviva; Moyal, Lilach; Crawford, Thomas O.; Lederman, Howard M.; Ziv, Yael; Shiloh, Yosef (2007): Ataxia-telangiectasia: mild neurological presentation despite null ATM mutation and severe cellular phenotype. In: *Am. J. Med. Genet. A* 143A (16), S. 1827–1834. DOI: 10.1002/ajmg.a.31853.

Angèle, S.; Hall, J. (2000): The ATM gene and breast cancer: is it really a risk factor? In: *Mutat. Res.* 462 (2-3), S. 167–178.

Bakkenist, Christopher J.; Kastan, Michael B. (2003): DNA damage activates ATM through intermolecular autophosphorylation and dimer dissociation. In: *Nature* 421 (6922), S. 499–506. DOI: 10.1038/nature01368.

Banin, S.; Moyal, L.; Shieh, S.; Taya, Y.; Anderson, C. W.; Chessa, L. et al. (1998): Enhanced phosphorylation of p53 by ATM in response to DNA damage. In: *Science* 281 (5383), S. 1674–1677.

Berge, Elisabet Ognedal; Staalesen, Vidar; Straume, Anne Hege; Lillehaug, Johan Richard; Lønning, Per Eystein (2010): Chk2 splice variants express a dominant-negative effect on the wild-type Chk2 kinase activity. In: *Biochim. Biophys. Acta* 1803 (3), S. 386–395. DOI: 10.1016/j.bbamcr.2010.01.005.

Berkovich, Elijahu; Monnat, Raymond J.; Kastan, Michael B. (2007): Roles of ATM and NBS1 in chromatin structure modulation and DNA double-strand break repair. In: *Nat. Cell Biol.* 9 (6), S. 683–690. DOI: 10.1038/ncb1599.

Bernstein, J. L.; Bernstein, L.; Thompson, W. D.; Lynch, C. F.; Malone, K. E.; Teitelbaum, S. L. et al. (2003): ATM variants 7271TG and IVS10-6TG among women with unilateral and bilateral breast cancer. In: *Br. J. Cancer* 89 (8), S. 1513–1516. DOI: 10.1038/sj.bjc.6601289.

Blum, Helmut; Beier, Hildburg; Gross, Hans J. (1987): Improved silver staining of plant proteins, RNA and DNA in polyacrylamide gels. In: *Electrophoresis* 8 (2), S. 93–99. DOI: 10.1002/elps.1150080203.

BODER, E. (1985): Ataxia-telangiectasia: an overview. In: *Kroc Found Ser* 19, S. 1–63.

BODER, E.; SEDGWICK, R. P. (1958): Ataxia-telangiectasia; a familial syndrome of progressive cerebellar ataxia, oculocutaneous telangiectasia and frequent pulmonary infection. In: *Pediatrics* 21 (4), S. 526–554.

Canman, C. E.; Lim, D. S.; Cimprich, K. A.; Taya, Y.; Tamai, K.; Sakaguchi, K. et al. (1998): Activation of the ATM kinase by ionizing radiation and phosphorylation of p53. In: *Science* 281 (5383), S. 1677–1679.

Chahrour, Osama; Cobice, Diego; Malone, John (2015): Stable isotope labelling methods in mass spectrometry-based quantitative proteomics. In: *Journal of pharmaceutical and biomedical analysis* 113, S. 2–20. DOI: 10.1016/j.jpba.2015.04.013.

Chenevix-Trench, Georgia; Spurdle, Amanda B.; Gatei, Magtouf; Kelly, Helena; Marsh, Anna; Chen, Xiaoqing et al. (2002): Dominant negative ATM mutations in breast cancer families. In: *J. Natl. Cancer Inst.* 94 (3), S. 205–215.

Chun, Helen H.; Sun, Xia; Nahas, Shareef A.; Teraoka, Sharon; Lai, Chih Hung; Concannon, Patrick; Gatti, Richard A. (2003): Improved diagnostic testing for ataxia-telangiectasia by immunoblotting of nuclear lysates for ATM protein expression. In: *Mol. Genet. Metab.* 80 (4), S. 437–443.

Collas P.: Isolation of nuclei from somatic cells. Online verfügbar unter http://www.collaslab.com/protocols.html.

Curry, C. J.; O'Lague, P.; Tsai, J.; Hutchison, H. T.; Jaspers, N. G.; Wara, D. et al. (1989): ATFresno: a phenotype linking ataxia-telangiectasia with the Nijmegen breakage syndrome. In: *Am. J. Hum. Genet.* 45 (2), S. 270–275.

Dittrich, W.; Ghode, W.: Flow-through chamber for photometers to measure and count particles in a dispersion medium. Veröffentlichungsnr: US3761187 A.

Durocher, D.; Jackson, S. P. (2001): DNA-PK, ATM and ATR as sensors of DNA damage: variations on a theme? In: *Curr. Opin. Cell Biol.* 13 (2), S. 225–231.

Easton, D. F. (1994): Cancer risks in A-T heterozygotes. In: *International journal of radiation biology* 66 (6 Suppl), S. 82.

Elmore, Susan (2007): Apoptosis: a review of programmed cell death. In: *Toxicologic pathology* 35 (4), S. 495–516. DOI: 10.1080/01926230701320337.

FitzGerald, M. G.; Bean, J. M.; Hegde, S. R.; Unsal, H.; MacDonald, D. J.; Harkin, D. P. et al. (1997): Heterozygous ATM mutations do not contribute to early onset of breast cancer. In: *Nat. Genet.* 15 (3), S. 307–310. DOI: 10.1038/ng0397-307.

Fousteri, Maria; Mullenders, Leon H. F. (2008): Transcription-coupled nucleotide excision repair in mammalian cells: molecular mechanisms and biological effects. In: *Cell research* 18 (1), S. 73–84. DOI: 10.1038/cr.2008.6.

Gatei, M.; Young, D.; Cerosaletti, K. M.; Desai-Mehta, A.; Spring, K.; Kozlov, S. et al. (2000): ATM-dependent phosphorylation of nibrin in response to radiation exposure. In: *Nat. Genet.* 25 (1), S. 115–119. DOI: 10.1038/75508.

Gatti, R. A.; Berkel, I.; BODER, E.; Braedt, G.; Charmley, P.; Concannon, P. et al. (1988): Localization of an ataxia-telangiectasia gene to chromosome 11q22-23. In: *Nature* 336 (6199), S. 577–580. DOI: 10.1038/336577a0.

Gatti, R. A.; Tward, A.; Concannon, P. (1999): Cancer risk in ATM heterozygotes: a model of phenotypic and mechanistic differences between missense and truncating mutations. In: *Molecular genetics and metabolism* 68 (4), S. 419–423. DOI: 10.1006/mgme.1999.2942.

Gilad, S.; Chessa, L.; Khosravi, R.; Russell, P.; Galanty, Y.; Piane, M. et al. (1998): Genotype-phenotype relationships in ataxia-telangiectasia and variants. In: *Am. J. Hum. Genet.* 62 (3), S. 551–561. DOI: 10.1086/301755.

Gillet, Ludovic C.; Navarro, Pedro; Tate, Stephen; Rost, Hannes; Selevsek, Nathalie; Reiter, Lukas et al. (2012): Targeted data extraction of the MS/MS spectra generated by data-independent acquisition: a

new concept for consistent and accurate proteome analysis. In: *Molecular & cellular proteomics : MCP* 11 (6), S. 16717. DOI: 10.1074/mcp.O111.016717.

Guo, Zhi; Kozlov, Sergei; Lavin, Martin F.; Person, Maria D.; Paull, Tanya T. (2010): ATM activation by oxidative stress. In: *Science* 330 (6003), S. 517–521. DOI: 10.1126/science.1192912.

Gutiérrez-Enríquez, Sara; Fernet, Marie; Dörk, Thilo; Bremer, Michael; Lauge, Anthony; Stoppa-Lyonnet, Dominique et al. (2004): Functional consequences of ATM sequence variants for chromosomal radiosensitivity. In: *Genes Chromosomes Cancer* 40 (2), S. 109–119. DOI: 10.1002/gcc.20025.

Herskowitz, I. (1987): Functional inactivation of genes by dominant negative mutations. In: *Nature* 329 (6136), S. 219–222. DOI: 10.1038/329219a0.

Hoppe-Seyler, F.; Butz, K.; Rittmüller, C.; Knebel Doeberitz, M. von (1991): A rapid microscale procedure for the simultaneous preparation of cytoplasmic RNA, nuclear DNA binding proteins and enzymatically active luciferase extracts. In: *Nucleic acids research* 19 (18), S. 5080.

Hu, Alex; Noble, William S.; Wolf-Yadlin, Alejandro (2016): Technical advances in proteomics. New developments in data-independent acquisition. In: *F1000Research* 5. DOI: 10.12688/f1000research.7042.1.

Huang, Da Wei; Sherman, Brad T.; Lempicki, Richard A. (2009a): Bioinformatics enrichment tools. Paths toward the comprehensive functional analysis of large gene lists. In: *Nucleic acids research* 37 (1), S. 1–13. DOI: 10.1093/nar/gkn923.

Huang, Da Wei; Sherman, Brad T.; Lempicki, Richard A. (2009b): Systematic and integrative analysis of large gene lists using DAVID bioinformatics resources. In: *Nature protocols* 4 (1), S. 44–57. DOI: 10.1038/nprot.2008.211.

Ikura, Tsuyoshi; Tashiro, Satoshi; Kakino, Akemi; Shima, Hiroki; Jacob, Naduparambil; Amunugama, Ravindra et al. (2007): DNA damage-dependent acetylation and ubiquitination of H2AX enhances chromatin dynamics. In: *Mol. Cell. Biol.* 27 (20), S. 7028–7040. DOI: 10.1128/MCB.00579-07.

Jager, M. de; van Noort, J.; van Gent, D. C.; Dekker, C.; Kanaar, R.; Wyman, C. (2001): Human Rad50/Mre11 is a flexible complex that can tether DNA ends. In: *Mol. Cell* 8 (5), S. 1129–1135.

Kastan, M. B.; Zhan, Q.; el-Deiry, W. S.; Carrier, F.; Jacks, T.; Walsh, W. V. et al. (1992): A mammalian cell cycle checkpoint pathway utilizing p53 and GADD45 is defective in ataxia-telangiectasia. In: *Cell* 71 (4), S. 587–597.

Khanna, K. K.; Keating, K. E.; Kozlov, S.; Scott, S.; Gatei, M.; Hobson, K. et al. (1998): ATM associates with and phosphorylates p53: mapping the region of interaction. In: *Nat. Genet.* 20 (4), S. 398–400. DOI: 10.1038/3882.

Kim, Seong-Tae; Xu, Bo; Kastan, Michael B. (2002): Involvement of the cohesin protein, Smc1, in Atm-dependent and independent responses to DNA damage. In: *Genes & development* 16 (5), S. 560–570. DOI: 10.1101/gad.970602.

Kitagawa, Risa; Bakkenist, Christopher J.; McKinnon, Peter J.; Kastan, Michael B. (2004): Phosphorylation of SMC1 is a critical downstream event in the ATM-NBS1-BRCA1 pathway. In: *Genes Dev.* 18 (12), S. 1423–1438. DOI: 10.1101/gad.1200304.

Knudson, A. G., JR (1971): Mutation and cancer: statistical study of retinoblastoma. In: *Proceedings of the National Academy of Sciences of the United States of America* 68 (4), S. 820–823.

Kozlov, Sergei V.; Graham, Mark E.; Peng, Cheng; Chen, Philip; Robinson, Phillip J.; Lavin, Martin F. (2006): Involvement of novel autophosphorylation sites in ATM activation. In: *EMBO J.* 25 (15), S. 3504–3514. DOI: 10.1038/sj.emboj.7601231.

Lavin, Martin F. (2008): Ataxia-telangiectasia: from a rare disorder to a paradigm for cell signalling and cancer. In: *Nat. Rev. Mol. Cell Biol.* 9 (10), S. 759–769. DOI: 10.1038/nrm2514.

Lim, D. S.; Kirsch, D. G.; Canman, C. E.; Ahn, J. H.; Ziv, Y.; Newman, L. S. et al. (1998): ATM binds to beta-adaptin in cytoplasmic vesicles. In: *Proc. Natl. Acad. Sci. U.S.A.* 95 (17), S. 10146–10151.

Llorca, O.; Rivera-Calzada, A.; Grantham, J.; Willison, K. R. (2003): Electron microscopy and 3D reconstructions reveal that human ATM kinase uses an arm-like domain to clamp around double-stranded DNA. In: *Oncogene* 22 (25), S. 3867–3874. DOI: 10.1038/sj.onc.1206649.

Lottspeich, Friedrich (2009): Introduction to proteomics. In: *Methods in molecular biology (Clifton, N.J.)* 564, S. 3–10. DOI: 10.1007/978-1-60761-157-8_1.

Lou, Zhenkun; Minter-Dykhouse, Katherine; Franco, Sonia; Gostissa, Monica; Rivera, Melissa A.; Celeste, Arkady et al. (2006): MDC1 maintains genomic stability by participating in the amplification of ATM-dependent DNA damage signals. In: *Mol. Cell* 21 (2), S. 187–200. DOI: 10.1016/j.molcel.2005.11.025.

Louis-Bar, D. (1941): Sur un syndrom progressif comprenant des télangiectasies capillaires cutanées et conjunctivals symétriques à disposition naevoide et des troubles cérébelleux. In: *Confin Neurol* (4), S. 32–42.

McConville, C. M.; Stankovic, T.; Byrd, P. J.; McGuire, G. M.; Yao, Q. Y.; Lennox, G. G.; Taylor, M. R. (1996): Mutations associated with variant phenotypes in ataxia-telangiectasia. In: *Am. J. Hum. Genet.* 59 (2), S. 320–330.

McFarlin, D. E.; Strober, W.; Barlow, M.; Waldmann, T. (1971): The immunological deficiency state in ataxia-telangiectasia. In: *Res Publ Assoc Res Nerv Ment Dis* 49, S. 275–292.

McFarlin, D. E.; Strober, W.; Waldmann, T. A. (1972): Ataxia-telangiectasia. In: *Medicine (Baltimore)* 51 (4), S. 281–314.

Meyer, Andreas; John, Esther; Dörk, Thilo; Sohn, Christof; Karstens, Johann H.; Bremer, Michael (2004): Breast cancer in female carriers of ATM gene alterations: outcome of adjuvant radiotherapy. In: *Radiother Oncol* 72 (3), S. 319–323. DOI: 10.1016/j.radonc.2004.07.010.

Miyamoto, Shigeki (2011): Nuclear initiated NF-kappaB signaling: NEMO and ATM take center stage. In: *Cell research* 21 (1), S. 116–130. DOI: 10.1038/cr.2010.179.

Nahas, Shareef A.; Butch, Anthony W.; Du, Liutao; Gatti, Richard A. (2009): Rapid flow cytometry-based structural maintenance of chromosomes 1 (SMC1) phosphorylation assay for identification of ataxia-telangiectasia homozygotes and heterozygotes. In: *Clin. Chem.* 55 (3), S. 463–472. DOI: 10.1373/clinchem.2008.107128.

Neuhoff, V.; Arold, N.; Taube, D.; Ehrhardt, W. (1988): Improved staining of proteins in polyacrylamide gels including isoelectric focusing gels with clear background at nanogram sensitivity

using Coomassie Brilliant Blue G-250 and R-250. In: *Electrophoresis* 9 (6), S. 255–262. DOI: 10.1002/elps.1150090603.

O'Farrell, P. H. (1975): High resolution two-dimensional electrophoresis of proteins. In: *The Journal of biological chemistry* 250 (10), S. 4007–4021.

Paull, Tanya T.; Lee, Ji-Hoon (2005): The Mre11/Rad50/Nbs1 complex and its role as a DNA double-strand break sensor for ATM. In: *Cell Cycle* 4 (6), S. 737–740.

Peterson, R. D.; Funkhouser, J. D. (1990): Ataxia-telangiectasia: an important clue. In: *N. Engl. J. Med.* 322 (2), S. 124–125. DOI: 10.1056/NEJM199001113220209.

Pilch, Duane R.; Sedelnikova, Olga A.; Redon, Christophe; Celeste, Arkady; Nussenzweig, Andre; Bonner, William M. (2003): Characteristics of gamma-H2AX foci at DNA double-strand breaks sites. In: *Biochem. Cell Biol.* 81 (3), S. 123–129. DOI: 10.1139/o03-042.

Porcedda, Paola; Turinetto, Valentina; Brusco, Alfredo; Cavalieri, Simona; Lantelme, Erica; Orlando, Luca et al. (2008): A rapid flow cytometry test based on histone H2AX phosphorylation for the sensitive and specific diagnosis of ataxia telangiectasia. In: *Cytometry A* 73 (6), S. 508–516. DOI: 10.1002/cyto.a.20566.

Rascle, Anne; Johnston, James A.; Amati, Bruno (2003): Deacetylase activity is required for recruitment of the basal transcription machinery and transactivation by STAT5. In: *Molecular and cellular biology* 23 (12), S. 4162–4173.

Renwick, Anthony; Thompson, Deborah; Seal, Sheila; Kelly, Patrick; Chagtai, Tasnim; Ahmed, Munaza et al. (2006): ATM mutations that cause ataxia-telangiectasia are breast cancer susceptibility alleles. In: *Nat. Genet.* 38 (8), S. 873–875. DOI: 10.1038/ng1837.

Rivera-Calzada, Angel; Maman, Joseph D.; Maman, Joseph P.; Spagnolo, Laura; Pearl, Laurence H.; Llorca, Oscar (2005): Three-dimensional structure and regulation of the DNA-dependent protein kinase catalytic subunit (DNA-PKcs). In: *Structure* 13 (2), S. 243–255. DOI: 10.1016/j.str.2004.12.006.

Roderick J. A. Little, Donald B. Rubin (2002): Statistical Analysis with Missing Data. 2nd Edition. New York: John Wiley & Sons (Wiley Series in Probability and Statistics).

Romeo, Francesco; Falbo, Lucia; Di Sanzo, Maddalena; Misaggi, Roberta; Faniello, Maria C.; Viglietto, Giuseppe et al. (2011): BRCA1 is required for hMLH1 stabilization following doxorubicin-induced DNA damage. In: *The international journal of biochemistry & cell biology* 43 (12), S. 1754–1763. DOI: 10.1016/j.biocel.2011.08.011.

Rubbi, C. P.; Milner, J. (2001): Analysis of nucleotide excision repair by detection of single-stranded DNA transients. In: *Carcinogenesis* 22 (11), S. 1789–1796.

Salton, Maayan; Lerenthal, Yaniv; Wang, Shih-Ya; Chen, David J.; Shiloh, Yosef (2010): Involvement of Matrin 3 and SFPQ/NONO in the DNA damage response. In: *Cell cycle (Georgetown, Tex.)* 9 (8), S. 1568–1576. DOI: 10.4161/cc.9.8.11298.

Saunders-Pullman, Rachel J.; Gatti, Richard (2009): Ataxia-telangiectasia: without ataxia or telangiectasia? In: *Neurology* 73 (6), S. 414–415. DOI: 10.1212/WNL.0b013e3181b39140.

Saviozzi, S.; Saluto, A.; Taylor, A. M.; Last, J. I.; Trebini, F.; Paradiso, M. C. et al. (2002): A late onset variant of ataxia-telangiectasia with a compound heterozygous genotype, A8030G/7481insA. In: *J. Med. Genet.* 39 (1), S. 57–61.

Savitsky, K.; Sfez, S.; Tagle, D. A.; Ziv, Y.; Sartiel, A.; Collins, F. S. et al. (1995): The complete sequence of the coding region of the ATM gene reveals similarity to cell cycle regulators in different species. In: *Hum. Mol. Genet.* 4 (11), S. 2025–2032.

Schaffner, W.; Weissmann, C. (1973): A rapid, sensitive, and specific method for the determination of protein in dilute solution. In: *Analytical biochemistry* 56 (2), S. 502–514.

Shahi, Ankita; Lee, Jung-Hee; Kang, Yoonsung; Lee, Sung Haeng; Hyun, Jin-Won; Chang, In-Youb et al. (2011): Mismatch-repair protein MSH6 is associated with Ku70 and regulates DNA double-strand break repair. In: *Nucleic acids research* 39 (6), S. 2130–2143. DOI: 10.1093/nar/gkq1095.

Shav-Tal, Yaron; Zipori, Dov (2002): PSF and p54(nrb)/NonO--multi-functional nuclear proteins. In: *FEBS letters* 531 (2), S. 109–114.

Simbürger, Johann M. B.; Dettmer, Katja; Oefner, Peter J.; Reinders, Joerg (2016): Optimizing the SWATH-MS-workflow for label-free proteomics. In: *Journal of proteomics* 145, S. 137–140. DOI: 10.1016/j.jprot.2016.04.021.

Stankovic, T.; Kidd, A. M.; Sutcliffe, A.; McGuire, G. M.; Robinson, P.; Weber, P. et al. (1998): ATM mutations and phenotypes in ataxia-telangiectasia families in the British Isles: expression of mutant ATM and the risk of leukemia, lymphoma, and breast cancer. In: *Am. J. Hum. Genet.* 62 (2), S. 334–345. DOI: 10.1086/301706.

Stewart, G. S.; Last, J. I.; Stankovic, T.; Haites, N.; Kidd, A. M.; Byrd, P. J.; Taylor, A. M. (2001): Residual ataxia telangiectasia mutated protein function in cells from ataxia telangiectasia patients, with 5762ins137 and 7271T--G mutations, showing a less severe phenotype. In: *The Journal of biological chemistry* 276 (32), S. 30133–30141. DOI: 10.1074/jbc.M103160200.

Sun, Xia; Becker-Catania, Sara G.; Chun, Helen H.; Hwang, Mee Jeong; Huo, Yong; Wang, Zhijun et al. (2002): Early diagnosis of ataxia-telangiectasia using radiosensitivity testing. In: *J. Pediatr.* 140 (6), S. 724–731. DOI: 10.1067/mpd.2002.123879.

Sun, Yingli; Jiang, Xiaofeng; Chen, Shujuan; Fernandes, Norvin; Price, Brendan D. (2005): A role for the Tip60 histone acetyltransferase in the acetylation and activation of ATM. In: *Proc. Natl. Acad. Sci. U.S.A.* 102 (37), S. 13182–13187. DOI: 10.1073/pnas.0504211102.

Sun, Yingli; Xu, Ye; Roy, Kanaklata; Price, Brendan D. (2007): DNA damage-induced acetylation of lysine 3016 of ATM activates ATM kinase activity. In: *Mol. Cell. Biol.* 27 (24), S. 8502–8509. DOI: 10.1128/MCB.01382-07.

Swift, M.; Morrell, D.; Massey, R. B.; Chase, C. L. (1991): Incidence of cancer in 161 families affected by ataxia-telangiectasia. In: *N. Engl. J. Med.* 325 (26), S. 1831–1836. DOI: 10.1056/NEJM199112263252602.

Syllaba, L., Henner, K. (1926): Contribution á l'indépendance de l'athétose double idiopathique et congenitale. Atteinte familiale, syndrome dystrophique, signe due réseau vasculaire conjonctival, intégrité psychique. In: *Rev Neurol*, S. 541.

Thompson, Deborah; Duedal, Silvia; Kirner, Jennifer; McGuffog, Lesley; Last, James; Reiman, Anne et al. (2005): Cancer risks and mortality in heterozygous ATM mutation carriers. In: *J. Natl. Cancer Inst.* 97 (11), S. 813–822. DOI: 10.1093/jnci/dji141.

Towbin, H.; Staehelin, T.; Gordon, J. (1979): Electrophoretic transfer of proteins from polyacrylamide gels to nitrocellulose sheets: procedure and some applications. In: *Proceedings of the National Academy of Sciences of the United States of America* 76 (9), S. 4350–4354.

Uziel, T.; Savitsky, K.; Platzer, M.; Ziv, Y.; Helbitz, T.; Nehls, M. et al. (1996): Genomic Organization of the ATM gene. In: *Genomics* 33 (2), S. 317–320. DOI: 10.1006/geno.1996.0201.

Vermes, I.; Haanen, C.; Reutelingsperger, C. (2000): Flow cytometry of apoptotic cell death. In: *Journal of immunological methods* 243 (1-2), S. 167–190.

Vermes, I.; Haanen, C.; Steffens-Nakken, H.; Reutelingsperger, C. (1995): A novel assay for apoptosis. Flow cytometric detection of phosphatidylserine expression on early apoptotic cells using fluorescein labelled Annexin V. In: *Journal of immunological methods* 184 (1), S. 39–51.

Waddell, Nic; Jonnalagadda, Jyoti; Marsh, Anna; Grist, Scott; Jenkins, Mark; Hobson, Karen et al. (2006): Characterization of the breast cancer associated ATM 7271TG (V2424G) mutation by gene expression profiling. In: *Genes Chromosomes Cancer* 45 (12), S. 1169–1181. DOI: 10.1002/gcc.20381.

Wang, Wei; Scali, Monica; Vignani, Rita; Spadafora, Antonia; Sensi, Elisabetta; Mazzuca, Silvia; Cresti, Mauro (2003): Protein extraction for two-dimensional electrophoresis from olive leaf, a plant tissue containing high levels of interfering compounds. In: *Electrophoresis* 24 (14), S. 2369–2375. DOI: 10.1002/elps.200305500.

Watters, D.; Kedar, P.; Spring, K.; Bjorkman, J.; Chen, P.; Gatei, M. et al. (1999): Localization of a portion of extranuclear ATM to peroxisomes. In: *J. Biol. Chem.* 274 (48), S. 34277–34282.

Watts, Jason A.; Morley, Michael; Burdick, Joshua T.; Fiori, Jennifer L.; Ewens, Warren J.; Spielman, Richard S.; Cheung, Vivian G. (2002): Gene expression phenotype in heterozygous carriers of ataxia telangiectasia. In: *Am. J. Hum. Genet.* 71 (4), S. 791–800. DOI: 10.1086/342974.

Wisniewski, Jacek R.; Zougman, Alexandre; Nagaraj, Nagarjuna; Mann, Matthias (2009): Universal sample preparation method for proteome analysis. In: *Nature methods* 6 (5), S. 359–362. DOI: 10.1038/nmeth.1322.

Wu, Zhao-Hui; Shi, Yuling; Tibbetts, Randal S.; Miyamoto, Shigeki (2006): Molecular linkage between the kinase ATM and NF-kappaB signaling in response to genotoxic stimuli. In: *Science* 311 (5764), S. 1141–1146. DOI: 10.1126/science.1121513.

Zhang, Ye; Rohde, Larry H.; Wu, Honglu (2009): Involvement of nucleotide excision and mismatch repair mechanisms in double strand break repair. In: *Current genomics* 10 (4), S. 250–258. DOI: 10.2174/138920209788488544.

Zhao, Junhua; Jain, Aklank; Iyer, Ravi R.; Modrich, Paul L.; Vasquez, Karen M. (2009): Mismatch repair and nucleotide excision repair proteins cooperate in the recognition of DNA interstrand crosslinks. In: *Nucleic acids research* 37 (13), S. 4420–4429. DOI: 10.1093/nar/gkp399.

Zhu, Xiaochun; Chen, Yuping; Subramanian, Raju (2014): Comparison of information-dependent acquisition, SWATH, and MS(All) techniques in metabolite identification study employing ultrahigh-

performance liquid chromatography-quadrupole time-of-flight mass spectrometry. In: *Analytical chemistry* 86 (2), S. 1202–1209. DOI: 10.1021/ac403385y.